

Review

A Review of the Application of Carbon Materials for Lithium Metal Batteries

Zeyu Wu, Kening Sun and Zhenhua Wang *

Beijing Key Laboratory of Chemical Power Source and Green Catalysis, School of Chemistry and Chemical Engineering, Beijing Institute of Technology, Beijing 100081, China

* Correspondence: wangzh@bit.edu.cn

Abstract: Lithium secondary batteries have been the most successful energy storage devices for nearly 30 years. Until now, graphite was the most mainstream anode material for lithium secondary batteries. However, the lithium storage mechanism of the graphite anode limits the further improvement of the specific capacity. The lithium metal anode, with the lowest electrochemical potential and extremely high specific capacity, is considered to be the optimal anode material for next-generation lithium batteries. However, the lifetime degradation and safety problems caused by dendrite growth have seriously hindered its commercialization. Carbon materials have good electrical conductivity and modifiability, and various carbon materials were designed and prepared for use in lithium metal batteries. Here, we will start by analyzing the problems and challenges faced by lithium metal. Then, the application progress and achievements of various carbon materials in lithium metal batteries are summarized. Finally, the research suggestions are given, and the application feasibility of carbon materials in metal lithium batteries is discussed.

Keywords: lithium metal batteries; carbon materials; composite anodes; current collectors



Citation: Wu, Z.; Sun, K.; Wang, Z. A Review of the Application of Carbon Materials for Lithium Metal Batteries. *Batteries* **2022**, *8*, 246. <https://doi.org/10.3390/batteries8110246>

Academic Editor: Junsheng Zheng

Received: 15 October 2022

Accepted: 15 November 2022

Published: 18 November 2022

Publisher's Note: MDPI stays neutral with regard to jurisdictional claims in published maps and institutional affiliations.



Copyright: © 2022 by the authors. Licensee MDPI, Basel, Switzerland. This article is an open access article distributed under the terms and conditions of the Creative Commons Attribution (CC BY) license (<https://creativecommons.org/licenses/by/4.0/>).

1. Introduction

The use of fossil fuels has made invaluable contributions to the development of human society. However, problems such as resource depletion and environmental pollution force human beings to develop new energy systems and adjust the energy structure [1]. New systems such as wind, hydro, solar, and fuel cells are expected to provide clean and sustainable energy for human society. As an effective way to store and transfer energy, electrochemical energy storage has gradually become an indispensable part of the transformation of energy structure [2,3]. Since the advent of lithium-ion batteries in the 19th century, they have become an irreplaceable energy storage device in various fields [4,5]. With the unremitting efforts of researchers, the safety performance, specific energy, and cycle life of lithium-ion batteries were greatly improved, but they are still far from meeting the development needs of electric vehicles and portable electronic devices [6,7]. The human pursuit of high specific energy, long life, and fast charging batteries has never stopped. In the current commercial lithium secondary batteries, high nickel cathode materials can provide a specific capacity of 220 mA h g⁻¹ and an energy density of 800 W h kg⁻¹ [8]. However, the intercalation cathode material is limited by the crystal volume and element quality. Its specific energy is difficult to further improve. In this case, research to improve the energy density of batteries has mainly focused on the anode side. Widely used graphite materials have low specific capacity and energy density (specific capacity 372 mA h g⁻¹, energy density 300–400 W h kg⁻¹). Lithium metal anodes with high specific capacity (3860 mA h g⁻¹ or 2061 mA h cm⁻³) are considered to be the best choice for next-generation lithium battery anodes [9–11]. In particular, Li-S and Li-O₂ batteries assembled with high specific energy cathodes such as S or O₂ can provide specific energies as high as 650 W h kg⁻¹ and 950 W h kg⁻¹, respectively.

Lithium metal anodes were extensively studied long before graphite anodes, but were not effectively used until now. There are three main problems faced by Li metal anodes: (1) The depositing/stripping of Li metal during cycling is accompanied by a huge change in its volume, which leads to changes in the internal pressure and structure of the battery. (2) The side reactions that occur continuously with the battery cycle consume the effective components in the electrode and the electrolyte, resulting in a decrease in the coulombic efficiency of the battery or even failure. (3) Lithium metal tends to grow dendrites in liquid electrolytes. The formation of lithium dendrites has serious consequences: the larger specific surface area leads to more reactions with the electrolyte; the fracture of dendrites during cycling will cause part of the lithium metal to detach from the collector and become “dead lithium”, resulting in a decrease in electrode capacity; dendrites may also penetrate the separator and contact the positive electrode to short-circuit the battery and cause thermal runaway. The above problems have become the bottlenecks that limit their commercialization [12,13]. Paul Albertus et al. [14] believe that the application of a lithium battery needs to maintain an average Coulomb efficiency of 99.98% in 1000 cycles to reach the commercial level, and the current lithium metal anode is still far from this goal.

After more than 40 years of continuous research and deepening understanding of lithium metal electrodes, various strategies to control dendrite growth and improve the efficiency of lithium metal electrodes were proposed. These strategies have made various modifications and designs mainly from the perspectives of electrolytes, separators, SEIs, current collectors, composite electrodes, and solid electrolytes.

Electrolyte regulation For the electrolyte development of the lithium metal battery, the composition and structure of SEI are mainly regulated by changing the lithium salts and additives in the electrolyte [15]. In recent years, high-concentration and localized high-concentration electrolytes based on a solvated structure design have obtained lithium metal batteries with high Coulombic efficiency by promoting the decomposition of anions and reducing the reduction of free solvents [16–20]. However, expensive lithium salts and diluents hinder its further application. In addition to forming SEI, the electrolyte can also inhibit the growth of lithium dendrites by forming an electrostatic screen shielding layer on the surface of the lithium metal electrode. Cs^+ , Rb^+ , and other cations can suppress the formation of lithium dendrites by adsorbing on the surface of lithium metal to form an electrostatic shielding layer, thereby enabling the uniform deposition of lithium metal [21,22].

Separator modification: In the design of the lithium metal battery separator, the main purpose is to improve its Young's modulus to suppress the growth of lithium dendrites and to design the separator with uniform pores to obtain uniform lithium ion flux [23–26]. In addition, immobilizing inorganic materials or organic groups on the separator can obtain separators with specific functions, which can improve the safety and cycling stability of lithium metal batteries [27,28]. Utilizing the pore structure of the separator can also assist in adjusting the solvation structure of the electrolyte to obtain a functionalized separator with a wide electrochemical stability window and a stable SEI structure [29].

Artificial SEI The composition and structure of the SEI film on the surface of Li metal electrodes can be directly and effectively adjusted in situ by changing the composition of the electrolyte [30]. Artificial SEI layers can also be constructed on Li metal surfaces by ex situ methods [31,32]. Various organic polymers, inorganics, and organic–inorganic composite SEIs can provide high mechanical properties to suppress dendrite growth, high lithium ion conductivity to reduce polarization, and thus, improve the stability of lithium metal electrodes during battery cycling [33–38].

Current collector design Electrodeposition of lithium metal is closely related to its current density, and a large specific surface area can effectively reduce the local current density to inhibit dendrite growth [39]. Adding lithiophilic or nucleation-inducing substances to the current collector can also reduce the nucleation overpotential or uniform Li metal deposition. Metals and carbon materials such as Cu and Ni with excellent electronic conductivity are the two most common current collector materials [40–42]. In addition,

carbon materials have the characteristics of light weight, high electronic conductivity, and easy modification and are one of the excellent current collectors for lithium metal anodes.

Solid-state electrolytes: Solid-state electrolytes mainly include organic polymer electrolytes, inorganic ceramic electrolytes, and organic–inorganic composite electrolytes [43–48]. Solid-state electrolytes are considered to be the technical direction with the most potential to enable lithium metal batteries to be applied. Solid-state electrolytes are believed to provide high modulus and migration numbers close to unity without causing lithium dendrite growth. However, in the research of organic and inorganic solid electrolytes, it is found that short circuit or thermal runaway caused by dendrite growth is still inevitable [49–51].

Various new materials and technologies were tried to solve the problems faced by lithium metal batteries, but the commercialization of lithium metal electrodes is still full of challenges. Compared to other materials, carbon materials have excellent electrical and thermal conductivity. Their structural plasticity and easy modification allow them to be designed in a variety of shapes and have specific functions. With the rise in materials science and nanotechnology, carbon materials of different dimensions (0–3D) and different scales (nano–millimeter) were developed and played a huge role in lithium metal batteries (Figure 1). In lithium metal batteries, carbon materials are mainly used as current collectors to disperse current and heat. In addition, carbon materials can also be used as additives or artificial SEI to participate in lithium metal electrodes to inhibit dendrite growth and improve battery life.

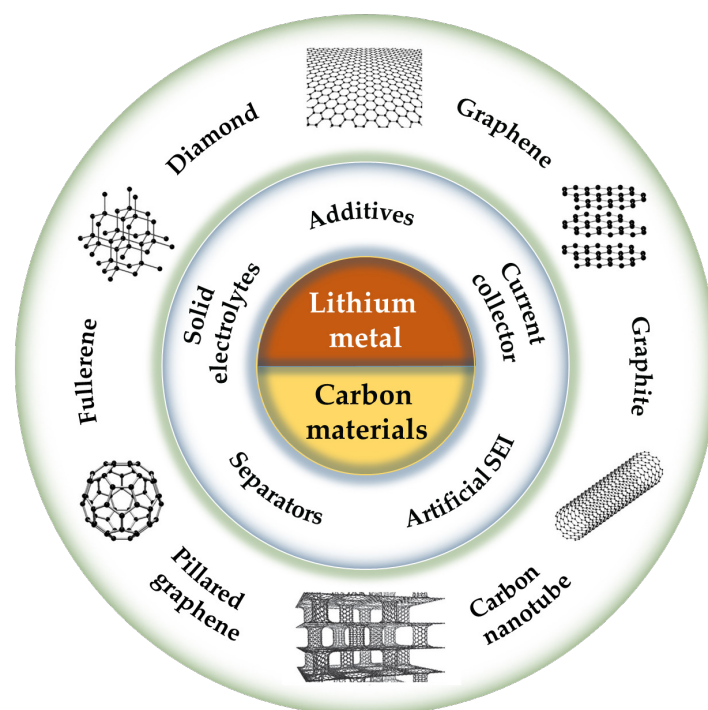


Figure 1. Various strategies applied by carbon materials in lithium metal batteries.

This review will start from the inherent scientific issues of metallic lithium anodes and introduce the problems and challenges of metallic lithium electrodes. Then, various applications of carbon and its derivatives/composites in lithium metal batteries are summarized. Finally, the research of carbon materials in lithium metal batteries is discussed and suggestions for its development direction are provided.

2. Issues and Challenges of Lithium Metal Anodes

2.1. Nucleation of Lithium Metal

Lithium metal anodes undergo reversible plating and stripping during battery cycling. In each charging process, lithium atoms go through a process from nucleation to

growth. The nucleation state and growth pattern of Li metal have a huge effect on its deposition/dendritic morphology.

The nucleation process of Li metal is controlled by the properties of the deposition substrate, multiphysics, and SEI. Yan et al. [52] compared the nucleation process of lithium metal on different metal substrates and found that there is an obvious overpotential when lithium metal is deposited on the surface of a copper current collector, that is, the energy used to overcome the heterogeneous nucleation (Figure 2a). In contrast, the deposition of Li metal on the Au surface first forms a Li-Au alloy above 0 V, and then, there is almost no nucleation overpotential during the deposition process below 0 V (Figure 2b). They also verified the deposition process of lithium metal on more than ten current collectors and proved that the properties of the current collector have a significant impact on the lithium metal nucleation process (Figure 2c,d).

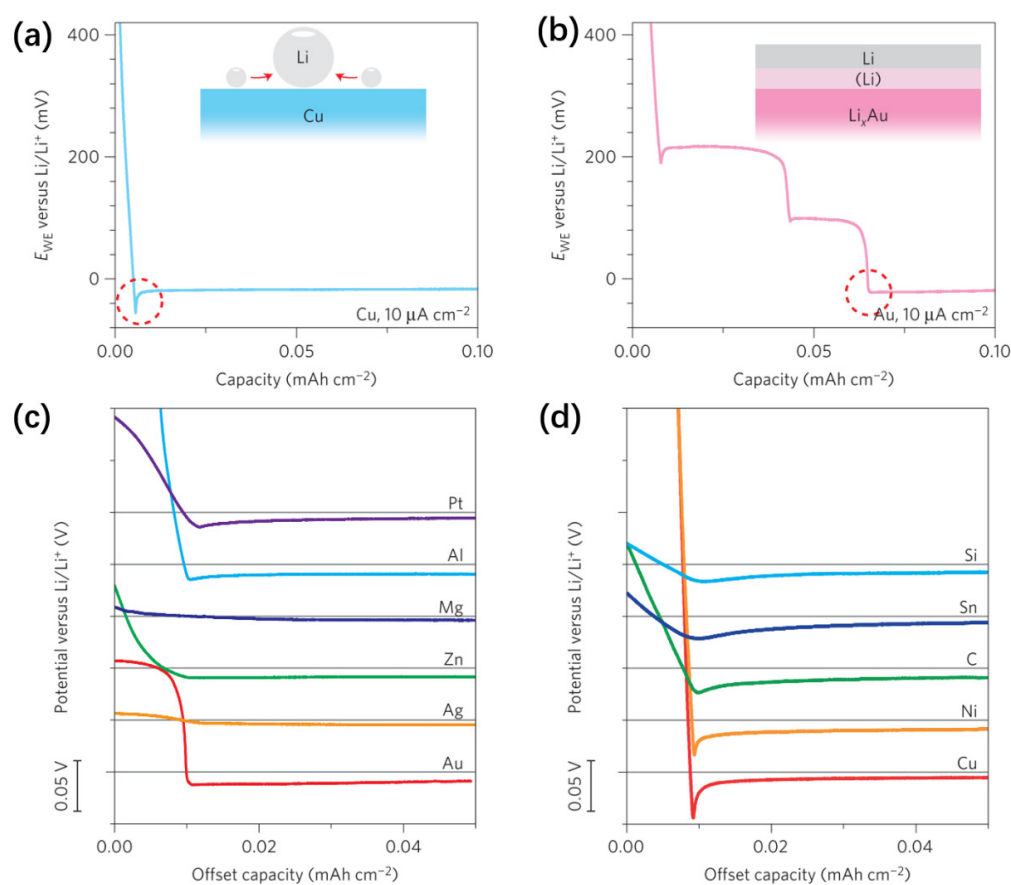


Figure 2. Voltage distributions of galvanostatic Li deposition on copper (a) and gold (b) substrates (E_{WE} is the potential of the working electrode) (c) Voltage distributions of various materials with a certain solubility in Li during Li deposition, (d) Displacement voltage distributions for various materials with negligible solubility in Li [52].

In addition to the properties of the deposition substrate, the presence of various physical fields can have an effect on the nucleation of lithium metal. Han et al. [39] observed the nucleation state of Li metal on copper substrates at different temperatures and current densities by SEM (Figure 3a). At low temperature and high current density, the nucleation density of Li metal is higher and the particles are smaller. Further, Pei et al. [53] combined the analysis of the homogeneous nucleation equation and the SEM experimental results to conclude that the size of the lithium metal nuclei is inversely proportional to the overpotential, and the nucleus number density is proportional to the third power of the overpotential (Figure 3b–d).

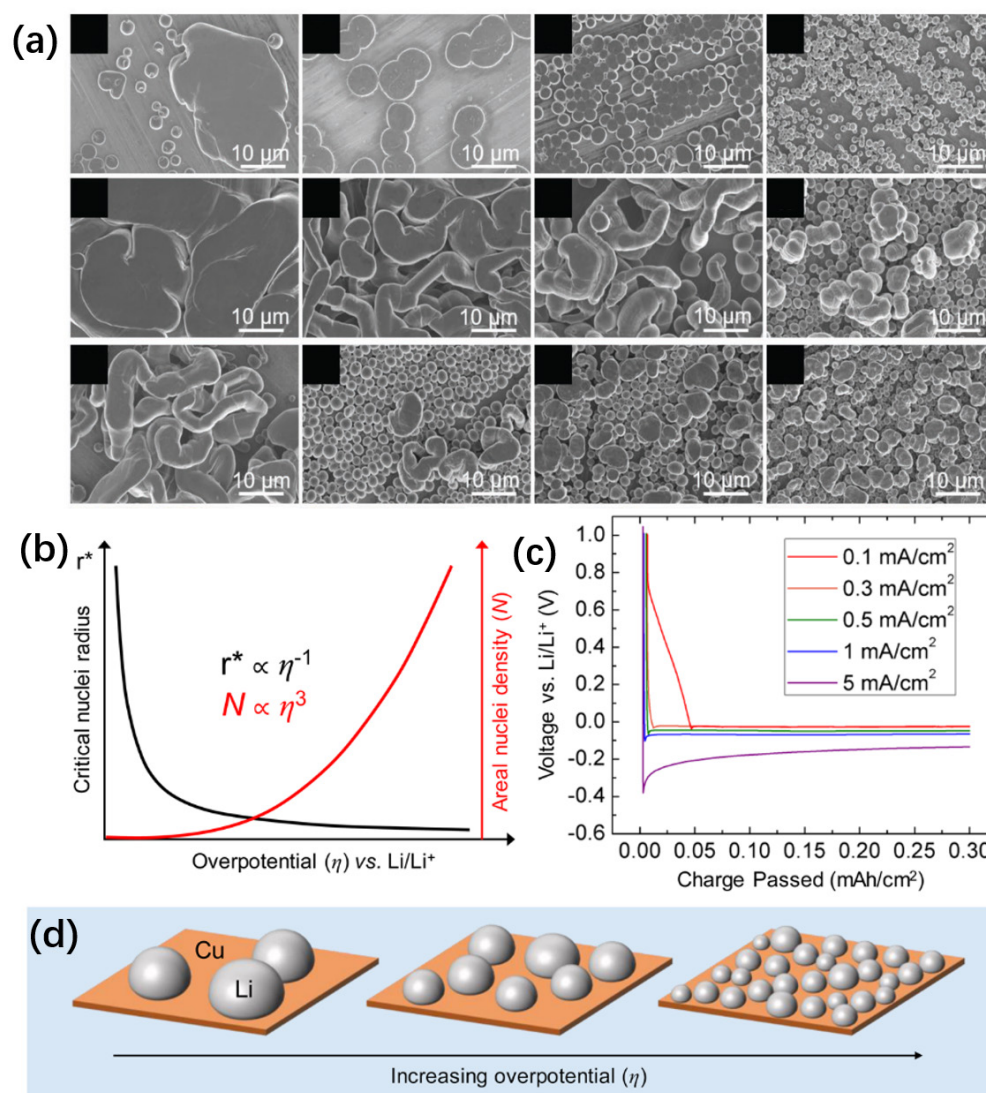


Figure 3. (a) Nucleation states of Li metal on copper substrates at different temperatures and current densities [39]. (b) Schematic diagram of the relationship between critical Li core radius and areal core density and Li deposition overpotential. (c) Experimental voltage distributions of Li deposition on Cu at different current densities. (d) Schematic illustration of the size and density of Li nuclei deposited on Cu at different overpotentials [53].

The use of lithium metal deposition materials with low nucleation overpotential and effective current density is an important way to regulate lithium metal nucleation. Carbon materials with high specific surface area and conductivity can effectively disperse the current density and, thus, make lithium metal deposition more uniform. Compared with metals such as Cu and Ni, carbon materials are lithiophilic. The lithiophilicity of carbon materials can be enhanced after doping or chemical treatment. Lithiophilic deposition substrates can induce more uniform nucleation and growth of lithium metals.

2.2. Growth of Dendrites and Formation of “Dead Lithium”

In terms of material properties, Li metal has a low surface energy and a high diffusion barrier (calculated about 0.14 eV [54]). During deposition, lithium metal tends to form a larger surface area to reach the lowest surface energy state. At the same time, lithium atoms have high diffusion energy on the bulk surface, which makes it difficult for atoms formed by lithium ions to obtain electrons to diffuse on the surface and form a uniform and flat structure. The natural properties of lithium metal determine that it tends to grow

one-dimensionally, that is, to grow into dendrites [55,56]. The growth of lithium dendrites is mainly affected by factors such as electric field strength, lithium ion flux, current density, temperature, and pressure [56]. The widely accepted space charge model can well explain the growth of Li dendrites in the liquid electrolyte. Chazalviel et al. [57] believed that the space charge layer in dilute solution led to the formation of dendrites. Specifically, at the initial stage of deposition, lithium ions on the electrode surface gain electrons and become atoms. However, the lithium ions in the convection region cannot reach the electrode surface quickly due to the slow diffusion rate, and a concentration gradient of lithium ions is formed on the electrode surface at this time. The existence of the concentration gradient resulted in the formation of a space charge layer on the electrode surface. At this time, the uneven surface of the electrode leads to uneven distribution of electrons at the interface. Under the combined action of the electric field and ion field, lithium ions will preferentially deposit at the protrusions (lithium metal nucleation sites or dendrite tip), a phenomenon also known as the “tip effect”. This growth mode is quantified by Sand and summarized as Sand’s Time formula to predict the critical condition for dendrite growth [58]:

$$\tau_s = \pi D \left(\frac{C_0 e z_c}{2J} \right)^2 \left(\frac{\mu_a + \mu_c}{\mu_a} \right)^2 \quad (1)$$

$$D = \frac{\mu_a D_c + \mu_c D_a}{\mu_a + \mu_c} \quad (2)$$

where e is the electron charge, J is the effective electrode current density, z_c is the number of cationic charges, and C_0 is the initial concentration of Li salt. μ_c and μ_a are the anion and cation (Li+) mobilities, D is the bipolar diffusion coefficient, D_c and D_a are the cation and anion diffusion coefficients.

It can be seen that reducing the current density can increase the onset time of lithium dendrite growth so as to achieve the effect of inhibiting the growth of dendrites. Yoon et al. [59] analyzed the relationship between the current density and deposition capacity of lithium metal and the growth of lithium dendrites and showed that with the increase in current density, the critical discharge required to form dendrites first increased and then decreased. In addition to current density, compressive stress is also an important factor controlling dendrite growth. Monroe and Newman predicted that shear moduli over 10^9 Pa could inhibit dendrite growth [60]. Temperature can affect the growth process and morphology of dendrites through the diffusion and surface reaction of Li ions. The study by Hitoshi Ota et al. [61] found that dendrite growth is more serious at a lower temperature.

In different electrolyte systems, dendrites appear with different morphologies, indicating that the morphology of lithium dendrites is also controlled by the electrolyte and the SEI derived from the electrolyte. The presence of defects induces Li metal deposition on current collectors or SEIs at defects, dislocations, grain boundaries, and even contaminants. Under the combined action of many influencing factors, lithium dendrites can appear as needle-like, mossy-like or tree-like. The growth of dendrites mainly leads to three adverse consequences: penetrating the separator and contacting the positive electrode, resulting in a short circuit or even thermal runaway of the battery; the larger specific surface area aggravates the reaction between the electrode and the electrolyte, which consumes the electrolyte in the battery; lithium dendrites form “dead lithium” after fracture, resulting in the loss of lithium inventory.

“Dead lithium” formed after lithium dendrites break cannot continue to participate in the electrochemical process because they are separated from the current collector. The loss of active material will lead to the decrease in battery capacity, and the large amount of “dead lithium” wrapped by SEI on the electrode surface will also hinder the mass transfer process and cause the increase in polarization. The composition of SEI and “dead lithium” in pulverized lithium anodes can be quantitatively analyzed by titrimetric gas chromatography [62] and nuclear magnetic resonance spectroscopy [63]. This study found

that the “dead lithium” that loses activity due to detachment from the current collector is an important factor leading to battery capacity decay.

In this case, the growth of lithium dendrites can be inhibited by reducing the effective current density. Carbon materials with high specific surface areas can disperse the current density, thereby reducing the local current density to obtain a dendrite-free lithium metal anode. At the same time, carbon materials with good mechanical strength as artificial SEI can also inhibit the growth of lithium dendrite.

2.3. Solid Electrolyte Interphase of Lithium Metal Anode

The solid electrolyte interphase (SEI) is a passivation interface layer formed by chemical and electrochemical reactions on the surface of the negative electrode. Similar to the solid-state electrolyte, the SEI acts to conduct lithium ions and block further reactions between the active material and the electrolyte. Lithium metal and the electrolyte will form an SEI film through a chemical reaction at the moment of contact. This is because the electrochemical window of general organic electrolytes is about 1–4.7 V (relative to Li metal potential), and the electrode potential of Li metal is lower than the reduction potential of electrolytes [64,65]. Goodenough et al. [2] explained this phenomenon using the molecular orbital theory. As shown, the thermodynamic stability of the electrolyte is determined by its lowest unoccupied orbital (LUMO) and highest occupied orbital (HOMO) (Figure 4). When the electrochemical potential of the electrode is higher than the LUMO or lower than the HOMO, the contact between the electrode and the electrolyte will no longer be a thermodynamically stable state. At this time, the electrode will react with the electrolyte to form SEI. The presence of SEI complies with the electrochemical potentials of the electrode and electrolyte so that no further reactions can take place.

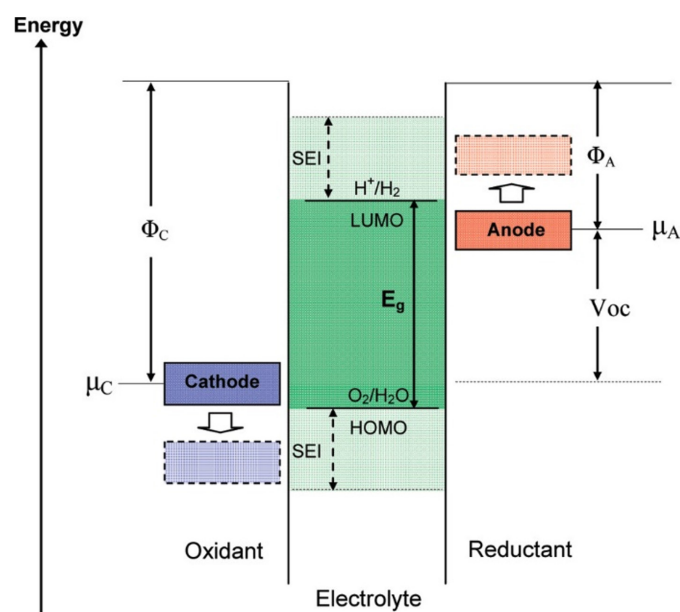


Figure 4. Schematic diagram of open circuit energy in liquid electrolytes. Φ_A and Φ_C are the anode and cathode working potentials, respectively. E_g is the electrolyte thermodynamic stability window. $\mu_A > \text{LUMO}$ and/or $\mu_C < \text{HOMO}$ indicate that the SEI layer needs to be formed to reach a kinetically stable state [2].

The native SEI formed by chemical reaction is often not enough to maintain stability during the electrochemical process, so the lithium metal electrode will also reduce the electrolyte through an electrochemical reaction to form SEI. During the electrochemical process, not only the new electrolyte is reduced to increase and thicken the SEI but the structure and composition of the original SEI also change. In addition, continuous cracking and regeneration of SEI also occurs due to the volume change and non-uniformity of

plating/stripping of Li metal. As shown in Figure 5, Cohen et al. [66] believed that during the deposition of lithium metal, the growth of lithium dendrites would also break the SEI, and the fresh lithium metal would continue to react with the electrolyte to form the SEI. When the lithium metal is peeled off, the brittle SEI film will rupture to expose the fresh lithium metal. At this time, the exposed lithium metal will continue to react with the electrolyte to form a new SEI.

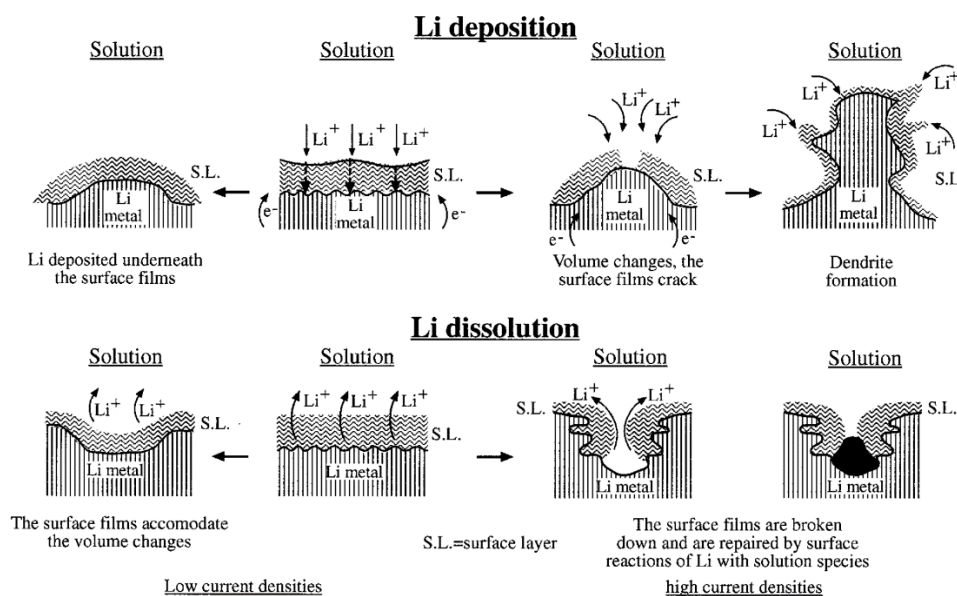


Figure 5. Description of the morphology and failure mechanism of Li electrodes during Li deposition and dissolution, with dendrite formation and heterogeneous Li dissolution accompanied by surface film destruction and repair [66].

The ideal SEI is believed to have high insulating properties, high lithium selectivity, and ionic conductivity; to be as thin as possible; with high strength and resistance to expansion and contraction stresses; to be insoluble in electrolytes; over a wide range of operating temperatures, and with stability under potential [67]. The active material and electrolyte components consumed to form the SEI lead to a decrease in battery capacity and even failure. The formation and evolution of SEI are affected by many factors, such as electrolyte composition, current collector material, temperature, electrolyte salt concentration, reduction current rate, side reactions, impurities, and uneven current distribution. The low thickness, complex structure, heterogeneous composition, and dynamic properties (spatial and temporal variations of morphology and composition) of SEI pose challenges to a comprehensive understanding of SEI [30].

With the development and innovation of characterization techniques, people's understanding of the structure and composition of SEI is constantly changing. Since SEI is an insoluble substance formed by the in situ reaction of lithium metal with the electrolyte, its chemical composition is dependent on the formulation of the electrolyte (salt anion, solvent, additives, concentration, and solvation structure). In addition, factors such as current density, cut-off voltage, capacity utilization, temperature, and pressure also have certain effects on the composition of SEI [30]. In the classic carbonate electrolyte with LiPF_6 as lithium salt, SEI is mainly composed of organic alkyl lithium carbonate (ROCO_2Li , $(\text{ROCO}_2\text{Li})_2$), inorganic lithium salts (LiF , Li_2CO_3 , Li_2O), and a small amount of fluorophosphate (LiPO_xF_y) [68–70]. There are three main models for the structure of SEI: the bilayer model [71], the mosaic model [72], and the mosaic pudding model [30,73] (Figure 6). Aurbach's analysis based on Raman, FTIR and XPS found that the SEI is a mixture of various organic and inorganic substances, and that the inorganic-rich inner layer (in contact with Li) and the organic-rich outer layer (in contact with the electrolyte) constitute the two-layer

structure of the SEI. The mosaic model believes that the SEI on the surface of lithium metal is composed of different lithium salts with mosaic-like morphology and stacking, and its inner layer is inorganic components, and the outer layer is mainly organic components. In recent years, based on the application of cryo-transmission electron microscopy, more researchers believe that the structure of SEI occurs when some single crystals of inorganic lithium salts are dispersed in an amorphous structure, and the first-principles density functional theory calculations and experiments have proven that amorphous regions and grain boundaries are the main routes for lithium ion transport [74].

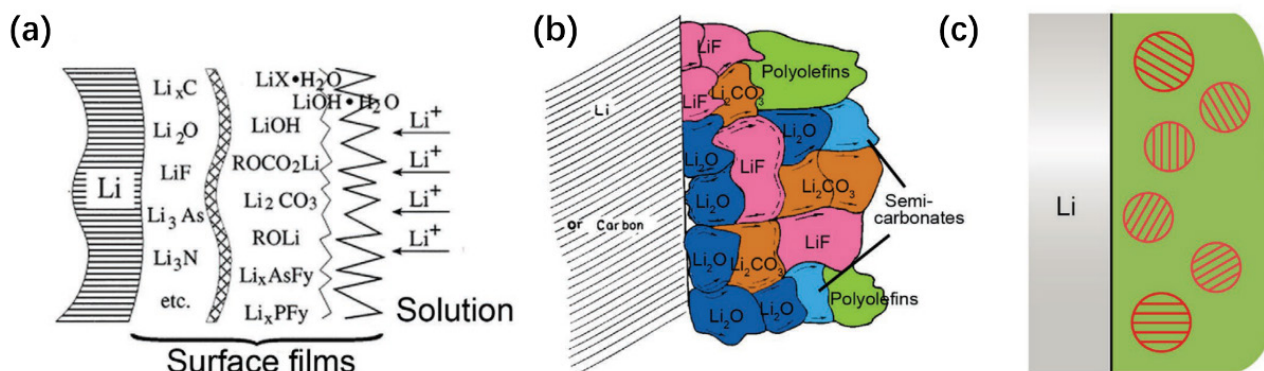


Figure 6. SEI model: (a) Multilayer model [71]; (b) Mosaic model [72]; (c) Raisin pudding model [30].

The regulation of the electrolyte directly affects the composition and structure of the anodes' SEI and is one of the simplest and most effective ways to improve the SEI. The design and use of an artificial SEI can compensate for the shortcomings of natural SEI and obtain a stable interface structure and dendrite-free lithium metal anode.

3. Recent Progress

3.1. Electrolyte Additives

The Fermi level of Li metal is lower than most common organic electrolytes, which leads to the inevitable reduction in Li salt and solvent molecules on the anode surface to form a solid electrolyte interphase (SEI). As an important component of the electrolyte, the use of additives can improve the various properties of anodes by forming SEI, changing the solvated structure, or changing the electric double layer structure [75–78].

Different from general electrolyte additives, carbon materials have electronic conductivity and can promote lithium metal nucleation when used as additives. Cheng et al. [79] used octadecylamine-treated nanodiamonds as additives in lithium metal batteries. Nanodiamonds with low diffusion barriers provide nucleation sites for Li metal, inducing the uniform deposition of Li metal. The nanodiamond-decorated electrolyte enables stable cycling of Li|Li symmetric cells at 2.0 mA cm^{-2} and 1.0 mA cm^{-2} for 150 h and 200 h, respectively. A Coulombic efficiency of 96% was obtained in Li|Cu cells. The addition of surfactants is bound to affect the battery. Hu et al. [80] added graphene quantum dots into the electrolyte to continuously control the growth morphology of lithium metal. Graphene quantum dots with a smaller size can be uniformly dispersed in the electrolyte without modification.

3.2. Separator Modification

In lithium batteries, the separator mainly functions to separate the electrodes and allow the electrolyte to pass through. It is a simple and valuable direction to improve lithium metal battery performance by modifying separators. Coating carbon materials on the separator surface is a simple and effective strategy. Carbon materials with higher mechanical strength has an inhibitory effect on dendrite growth. In addition, the porous carbon material with high specific surface area can control the lithium ions passing through the separator to be uniformly redistributed and, thus, deposit uniformly on the electrode

surface. For example, Xu et al. [81] used carbon nanosheet coatings with cubic cavities to suppress dendrite growth (Figure 7a,b). Connected cubic carbon channels enable stable Li metal battery cycling by modulating Li deposition behavior. Li|Li symmetric cells cycled for over 2600 h at 6 mA cm^{-2} and 2 mA h cm^{-2} , while Li|Cu cells achieved an average Coulombic efficiency of 98.5% at 2 mA cm^{-2} and 2 mA h cm^{-2} . Li et al. [82] coated a thin layer of ultra-strong diamond-like carbon (DLC) on the negative side of the polypropylene (PP) separator (Figure 7c). The coating not only has a high modulus to inhibit the growth of lithium dendrites but also undergoes in situ chemical lithiation with lithium metal in the battery, transforming into an excellent three-dimensional lithium ion conductor to redistribute lithium ion flux. The dual role of the DLC/PP separator enables the Li|Li symmetric cell to achieve stable cycling for over 4500 h at a current density of 3 mA cm^{-2} . Wang et al. [83] coated carbon fibers on the surface of separators for lithium metal batteries. The presence of carbon fibers improves the spatial electric field on the Li metal electrode surface and effectively suppresses the tip effect during dendrite growth. This study also provides new insights into the mechanism of action of carbon materials to modify the separator.

There are a large number of functional groups on the surface of carbon nanomaterials such as graphene oxide, and chemical reactions can be used to modify or modify these functional groups to obtain materials with specific functions. Li et al. [25] coated polyacrylamide-grafted graphene oxide nanosheets (GO-g-PAM) on one side of a commercial PP separator (Figure 7d). The robust GO backbone improves the mechanical strength, and the brush-like PAM chains on the graphene oxide surface contain a large number of polar groups such as C=O, N-H, etc., which provide functions for the efficient adhesion and uniform distribution of Li ions at the molecular level. Furthermore, the gaps between the stacked 2D molecular brushes provide a fast pathway for electrolyte diffusion. Liu et al. [84] coated the surface of the separator with functionalized nanocarbons modified with lithium p-benzenesulfonate groups and stabilized the deposition of lithium metal by inducing the opposite growth of lithium dendrites from the current collector and the separator (Figure 7e). In Li|LFP coin cells, this method can achieve long-term stable cycling (800 cycles with 80% initial capacity retention and 97% Coulombic efficiency).

3.3. Artificial SEI

The native SEI on the surface of Li metal electrodes is often difficult to adapt to the huge volume changes and electrochemical reactions of the electrodes during cycling. An artificial SEI used in situ and ex situ was designed to obtain a more stable interface structure. Carbon materials have good mechanical strength and good chemical/electrochemical stability. Carbon materials with different structures and their composites are designed as an artificial SEI to stabilize the electrode–electrolyte interface.

Cui et al. [37] used a monolayer of interconnected amorphous hollow carbon nanospheres as an artificial SEI layer to cover the Li metal surface (Figure 8a,b). The highly insulating top surface of the hollow carbon nanospheres promotes the deposition of metallic Li under the carbon nanospheres. The carbon layer as SEI can easily adapt to the volume change of Li metal during cycling. The Li|Cu half-cell assembled with ether electrolyte maintained a Coulombic efficiency of 99% for 150 cycles at a current density of 1 mA cm^{-2} and an areal capacity of 1 mA h cm^{-2} .

Graphene has excellent mechanical properties. The presence of defects and functional groups gives it excellent processability properties. Graphene and its derivatives or composites have received extensive attention as strategies for artificial SEI-stabilized lithium metal anodes [85–87]. Zhou et al. [88] covered the Li metal surface with several layers of parallel aligned graphene (Figure 8c). Flexible graphene films can adapt to the volume change of lithium metal during cycling. The Li|Li symmetric cell with this artificial SEI can operate for 1000 h at a current density of 5 mA cm^{-2} and a deposition capacity of 2.5 mA h cm^{-2} .

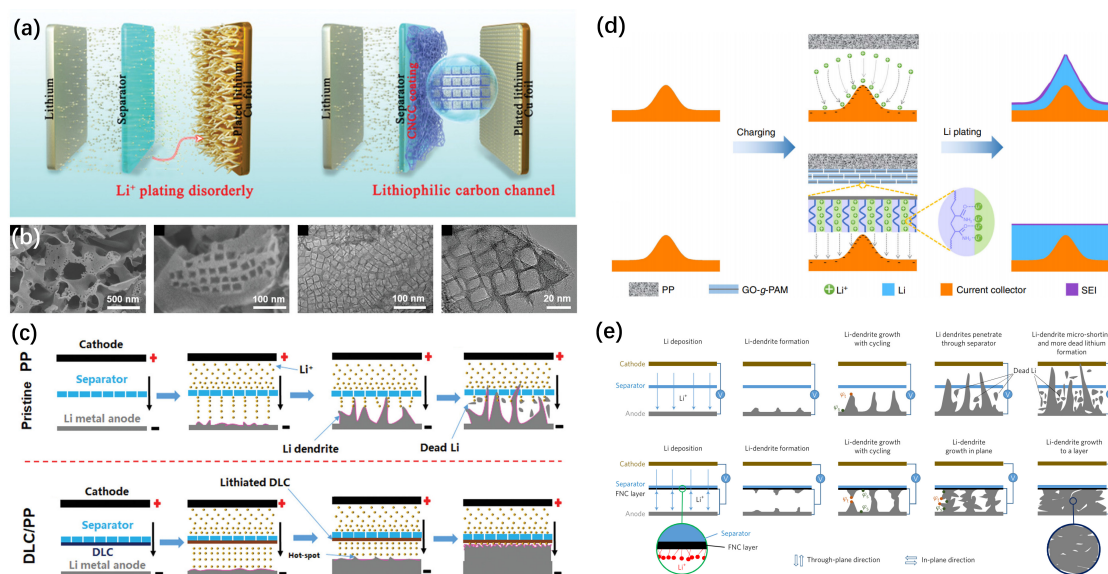


Figure 7. (a) Schematic illustration of Li-ion deposition in batteries with pristine separators or CNCC-coated separators. (b) SEM and TEM images of the CNCC coating [81]. (c) Schematic illustration of Li dendrite growth in pristine PP and LMB based on DLC/PP separator [82]. (d) Schematic illustration of Li ion deposition on electrodes with microscopic surface roughness [25]. (e) Growth of dendrites in blank cells and FNC cells [84].

Benefiting from the simple preparation process and good modification properties of graphene, a graphene artificial SEI combined with three-dimensional current collectors can provide higher Coulombic efficiency for lithium metal batteries. Xie et al. [89] grew graphene on the surface of nickel foam by chemical vapor deposition (CVD), and lithium metal was uniformly deposited between the nickel foam and graphene (Figure 8d). The graphene-based artificial SEI layer can inhibit the growth of dendrites and improve the cycling stability of the battery. On this basis, Wang et al. [35] composited graphene oxide and P(SF-DOL) to form an artificial SEI layer. The addition of polymers with Li-ion conductivity provides the artificial SEI with flexibility and Li-ion conductivity (Figure 8e). Combined with the three-dimensional copper foam current collector, the lithium metal battery protected by this artificial SEI maintains an average Coulombic efficiency of 99.1% over 300 cycles at a current density of 4.0 mA h cm^{-2} and a deposition capacity of 2.0 mA cm^{-2} (Figure 8f). In addition, graphene can also be composited with Prussian blue [90], LiF [91], etc. as artificial SEI layers to obtain dendrite-free Li metal batteries.

3.4. Current Collector Design

3.4.1. Lithium Metal Anode Using Carbon Material as Current Collector

As an important component of lithium batteries, current collectors not only play the role of transferring electrons between active materials and external circuits but also diffuse the heat generated inside the battery [92]. Meanwhile, the 3D current collector design can not only tolerate the huge volume change of Li metal during cycling but also achieve uniform Li deposition by reducing the current density. The properties of current collectors play an important role in the nucleation and deposition morphology of Li metal. Compared with metal materials, carbon materials have the advantages of low specific gravity and high abundance, as well as excellent electronic conductivity and lithiophilicity [93]. Thanks to their good plasticity and modifiability, various scales and various functionalized carbon materials were designed as current collectors for lithium metal batteries [94–98]. The large specific surface area can effectively reduce the local current density. At the same time, the lithiophilicity of carbon materials can be improved through surface modification to induce the uniform deposition of lithium metal. According to the morphological characteristics of the carbon material monomer, it can be divided into several categories from 0D to 3D.

Among them, 0D carbon materials mainly include carbon spheres, carbon nanoparticles, carbon quantum dots, etc.; 1D carbon materials mainly include carbon nanotubes, carbon nanowires, carbon fibers, etc.; 2D materials mainly include graphene, carbon nanosheets, etc.; 3D materials mainly include porous carbon, aerogel, and three-dimensional structures built from various carbon materials. Studies using carbon of different dimensions as current collectors are summarized and listed in Table 1.

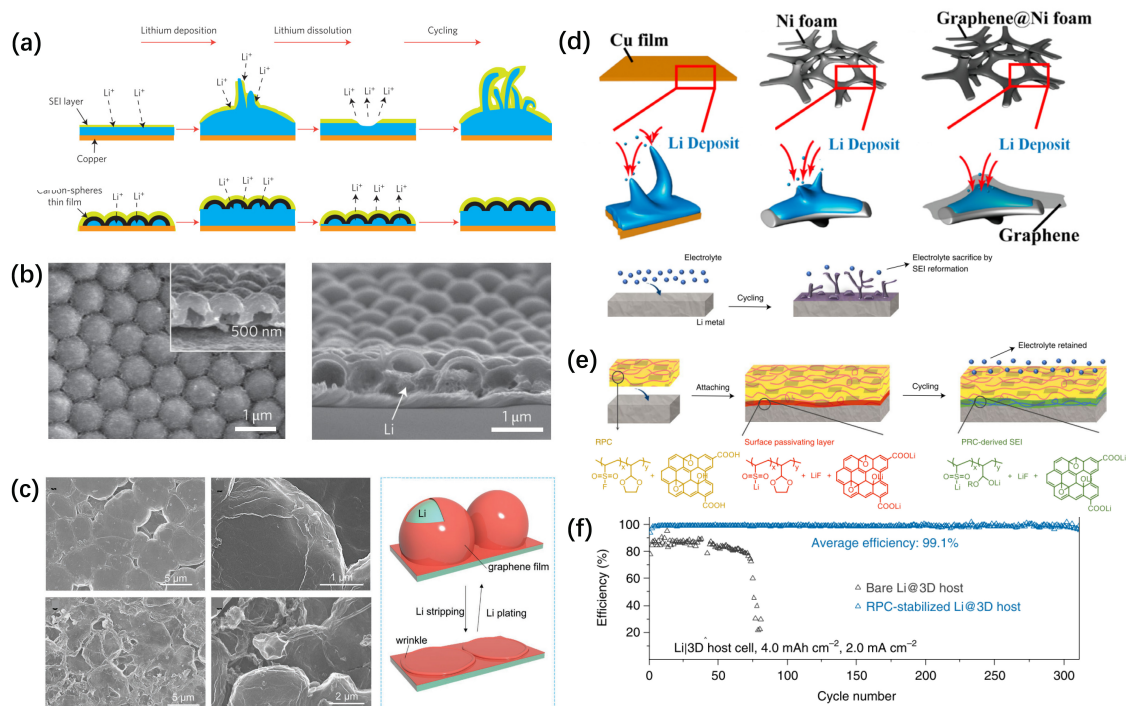


Figure 8. (a) Schematic illustration of the deposition of lithium metal in the presence of a stable SEI layer created by the hollow carbon nanosphere layer-modified copper substrate. (b) SEM image of hollow carbon nanospheres after initial SEI formation [37]. (c) Morphological changes and schematic diagrams of graphene films on Li metal anodes [88]. (d) Schematic illustration of Li deposition on bare copper foil, nickel foam, and 3D graphene@Ni foam. (e) Schematic illustration of molecular-level design of polymer-inorganic SEI using reactive polymer composites [89]. (f) Efficiency of Li|Cu 3D cells with RPC artificial SEI protection at a capacity of 4.0 mA h cm⁻² [35].

Table 1. Performance of lithium metal batteries using carbon materials as current collectors.

	Current Collector	Half Cell Performance (Cycle Number/h, CE)	Operating Conditions (Current Density/mA·cm ⁻² , Areal Capacity/mA h·cm ⁻²)	Reference
0D	Au@hollow carbon sphere	300, 98%	0.5, 1	[52]
	S-doped carbon nanospheres	220, ~97.5 %	0.5, 1	[99]
	Nitrogen-doped hollow porous carbon spheres	270, 98.5%	1, 1	[100]
	hollow carbon spheres modified with evenly dispersed Ni ₂ P nanoparticles	400, 98.4%	1, 1	[101]
1D	graphitic carbon tubes	350, 99.3%	0.5, 1	[102]
	hollow carbon fiber	350, 99.5%	0.5, 2	[103]
	Lotus-root-like Ni–Co hollow prisms@carbon fibers	250, 98%	3, 1	[104]
	Li/carbon nanotube hybrid	150, 95%	1, 0.5	[105]
	hollow carbon fiber	350, 99.5%	0.5, 2	[106]
	oxygen-rich carbon nanotube	200, 99%	2, 1	[107]

Table 1. Cont.

2D	layered reduced graphene oxide	-	-	[108]
	oxygen-codoped vertical carbon nanosheet arrays	325, 98%	0.5, 1	[109]
	S-doped graphene	180, 98.23%	1, 0.5	[110]
	3D fluorine-doped graphene	150, 98%	2, 1	[111]
3D	Nitrogen-doped amorphous Zn-carbon multichannel fibers decorated with carbon cages	800, 98%	1, 1	[112]
	Au nanoparticles@graphene hybrid aerogel	175, 91.2%	1, 1	[113]
	Carbon nanofiber-stabilized graphene aerogel film	100, 98.5%	3, 1	[114]

Although different morphologies of carbon materials can be used as current collectors for lithium metal electrodes, in order to obtain large specific surface area and porosity, most strategies are to design materials into 3D structures. The 3D carbon structure provides a larger specific surface area to reduce local current density, higher porosity, and mechanical strength to accommodate the volume change in Li metal during deposition and exfoliation. Infusion of molten lithium metal into 3D current collectors is the most common method, but this also requires the current collector itself to have a certain lithiophilicity [115]. Lin et al. [108] obtained graphene oxide films with good lithiophilicity through Li-assisted reduction vacuum filtration and then injected molten lithium into the uniform nano-gap of the graphene films (Figure 9a). The layered graphene can not only adapt to the huge volume change of Li metal but also stabilize the deposition and interface structure of Li metal. The mass fraction of graphene in the electrode is only 7%, which ensures the high specific capacity of the electrode.

In addition to the simple use of carbon materials to build 3D conductive frameworks, the modification of carbon materials and their surfaces can obtain current collector materials with special functions. Modification methods mainly include: doping, deposition, and chemical group modification.

Doping is a common means of modifying carbon materials. Elements such as N, O, and S can be doped into carbon materials to improve their lithiophilicity. Zhang et al. [116] designed a N, S co-doped ordered mesoporous carbon nanospheres as a deposition substrate for Li metal electrodes. The experimental and computational results show that the synergistic effect of N/S double doping enhances the surface electronegativity of the carbon spheres and lowers the nucleation energy barrier of Li-Au on the surface of the carbon spheres, enabling uniform nucleation in the initial stage, thereby inducing branch-free crystalline Li deposition. At the same time, N and S elements also help to form a more stable SEI layer, which prolongs the cycle life (400 h) of lithium metal symmetric batteries at high current density (20 mA h cm^{-2}).

In addition to doping, loading lithiophilic metal materials on the surface of carbon materials can induce nucleation and reduce overpotential [117,118]. Li et al. [119] and Tian et al. [120] coated the carbon cloth with Au and Ag layers, respectively, and then placed the metal-coated side away from the separator when assembling the battery. Lithium metal preferentially nucleates and grows at the metal coating during deposition. At the same time, the upper part of the porous skeleton of the carbon cloth also provides enough space to buffer the volume expansion of metallic lithium.

There are a large number of active functional groups on the surface of carbon materials such as graphene oxide and carbon nanotubes. Using these active sites to design chemical reactions can obtain carbon materials with specific functions. For example, Gao et al. [121] introduced benzenesulfonyl fluoride molecules on the surface of reduced graphene oxide aerogels (Figure 9b). During the metal deposition process, the labile molecules not only generate metal-coordinated benzenesulfonate anions to guide homogeneous metal deposition but also introduce lithium fluoride into the SEI to improve the SEI composition on the Li surface. High-efficiency lithium deposition with low nucleation overpotential is achieved at a current density of 6.0 mA cm^{-2} . Niu et al. [106] designed a lithium anode structure

based on an amine-functionalized mesoporous carbon fiber framework (Figure 9c). The introduction of amine groups enhanced the wettability of carbon fibers to lithium metal, which enabled the smooth deposition of lithium metal on the surface of carbon fibers. The full cell assembled with this anode can maintain stable cycling for 200 cycles at a low N/P ratio (< 2).

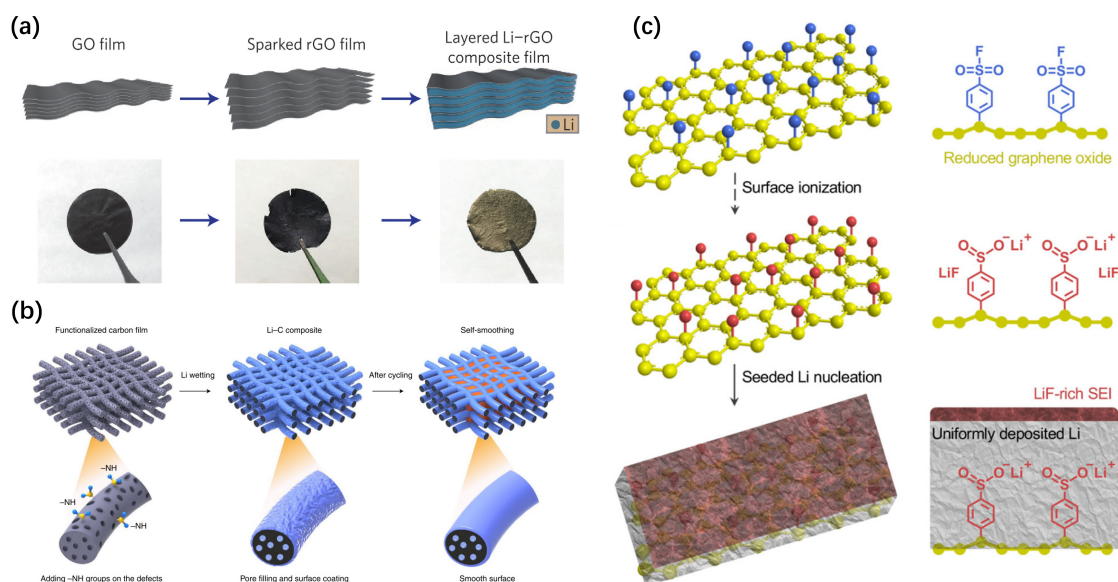


Figure 9. (a) Preparation of the layered Li-rGO composite film [108]. (b) Schematic illustration of the stabilized lithium deposition interface using the active organic molecule benzenesulfonyl fluoride (BSF) [121]. (c) Schematic illustration of the self-smoothing behavior of the lithium-carbon anode [106].

It is worth noting that either excess Li metal or excessively heavy current collectors will weaken or even offset the advantages of Li metal's high specific energy. Therefore, the design of thin and light and lithium-lean/lithium-free anodes has practical application value. The design of the 3D current collector is one of the most widely used and promising solutions for carbon materials in lithium metal batteries.

3.4.2. Graphite-Lithium Metal Composite Electrode

In recent years, a graphite-lithium metal composite electrode was proposed to simultaneously obtain the intercalation capacity of the graphite anode and the conversion capacity of the lithium metal by depositing a certain amount of lithium metal on the graphite electrode [122]. The use of 3D porous graphite hosts is expected to alleviate the volume expansion and dendrite growth problems of Li metal. Compared with the general lithium metal anodes using metal or carbon materials as current collectors, LiC_6 formed by graphite intercalation is considered to have good lithiophilicity [123]. Lithium metal can obtain lower nucleation overpotential on the surface of LiC_6 , resulting in more uniform deposition. In addition, the current collector material occupies more mass and volume in the electrode, which weakens the advantage of the high specific volume of the metal lithium electrode. The use of graphitized carbon materials with lithium intercalation ability combined with lithium metal is expected to break the capacity limitation of graphite anodes and provide electrodes with higher effective capacity. It is worth noting that ordinary lithium metal batteries often use an excess of lithium metal as the negative electrode, thereby ignoring the volume/mass ratio of the negative electrode in the battery. The lithium-free design of the composite anode is expected to improve the specific capacity of the full cell. From a practical point of consideration, the graphite-lithium metal composite electrode uses a commercial graphite anode as the lithium deposition substrate without changing the existing production process. Graphite has the advantages of high abundance and low cost,

and the use of graphite as the deposition substrate of lithium metal has high application feasibility. The design of the composite electrode is actually a compromise between the advantages and disadvantages of graphite and lithium metal. The specific capacity of graphite is improved while maintaining the stability and safety.

Although graphite-lithium metal composite anodes have many advantages compared with graphite anodes or lithium metal anodes, they also face many difficulties and challenges. Graphite was intensively researched and widely used as a mature lithium-ion battery anode. After Li metal is deposited on the graphite surface, the excess Li coating quickly fails in common carbonate-based electrolytes, resulting in a rapid decrease in battery capacity [124].

Graphitized carbon materials with various structures and functions have begun to be used as active substrates for lithium metal. These graphitic materials mainly function as 3D current collectors in electrodes [125]. A composite electrode with a higher capacity was obtained by depositing lithium metal into the voids of artificial graphite by Cui et al. (Figure 10a) [126]. Wan et al. [125] deposited Li metal on a 3D framework wrapped by graphitized carbon spheres, and the full cell assembled with LiFePO_4 achieved a lifespan of 1000 cycles using an anode with 5% Li pre-deposited by electrochemistry. Zuo et al. [127] reported that the graphitized carbon fiber electrode can be used as a multifunctional 3D current collector to enhance the lithium storage capacity. Intercalation and electrodeposition reactions can provide areal capacities up to 8 mA h cm^{-2} without significant dendrite formation.

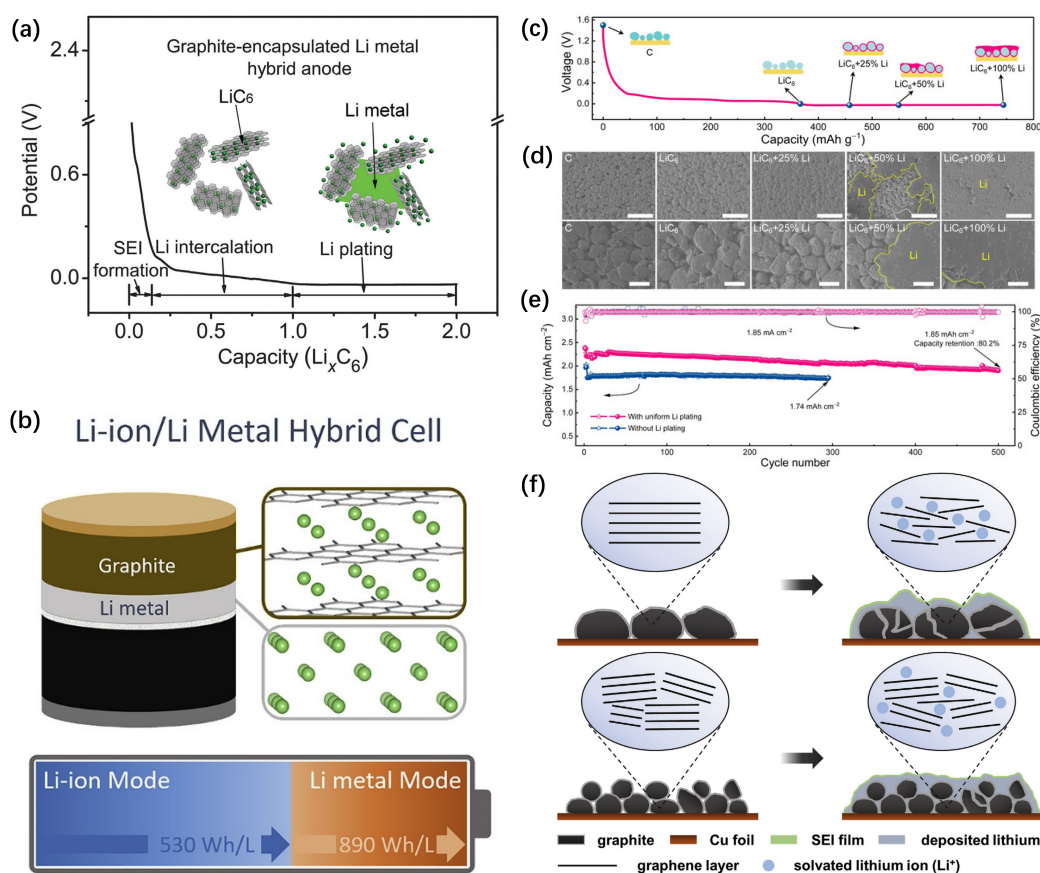


Figure 10. (a) Voltage variation of Li metal deposition in bulk artificial graphite [126]. (b) Schematic and specific energy of the hybrid Li-ion/Li-metal battery [122]. (c,d) Characterization of the morphological evolution of lithium intercalation and electroplated graphite electrodes. (e) Electrochemical performance of the lithium-graphite composite battery with localized highly concentrated electrolyte [128]. (f) Schematic illustration of the effects of NG and BMG structures on Li deposition and carbon structure evolution [129].

However, the research on graphite–lithium metal electrodes often ignores the capacity contribution of graphite itself, which also makes the volume-specific energy advantage of composite anodes not effectively utilized. In recent years, Dahn et al. [122] proposed the concept of lithium ion–lithium metal composite batteries. They believe that the use of graphite–lithium metal composite anode can increase the volume energy density of the anode from 530 W h L^{-1} to 890 W h L^{-1} (Figure 10b). However, the composite anode used by Dahn mainly deposits lithium on the surface of graphite to form a double-layer structure, and no further studies on the distribution of lithium were carried out. Zhang et al. [128] explored the boundary values for Li plating on graphite (Figure 10c–e). Combined with thermal monitoring, SEM, TOF-SIMS, and other characterizations, the properties of graphite–lithium metal electrodes with different lithium contents were tested. Their results show that the electrode surface has the most uniform lithium distribution when depositing lithium metal with a graphite capacity of 25%. Of course, the boundary value is affected by many conditions such as temperature, magnification, porosity, etc., and more work is needed to verify.

From a material point of view, reducing the particle size of graphite is considered to be more effective to obtain a more stable structure and a larger specific surface area (Figure 10f) [129]. The study of Chen et al. [124] showed that the capacity attenuation of graphite–lithium metal composite anodes mainly comes from the accumulation of dead lithium and the decrease in graphite capacity. The results of in situ X-ray microtomography analysis also confirmed this statement [130]: the main reason for the decrease in capacity after lithium deposition from graphite is that the graphite under the lithium metal layer is affected by mass transfer and cannot achieve the effective intercalation of lithium ions.

The focus of graphite–lithium metal composite anode research is on the construction of stable SEI and the maintenance of battery capacity. In order to construct a more robust SEI, Wu et al. [131] obtained a graphite–lithium metal composite anode with a longer cycle life by coating PVDF on the surface of the graphite electrode. By changing the carbon matrix or electrolyte, a uniform and stable in situ SEI can be effectively constructed. Wang et al. [132] fluorinated the edge of mesocarbon microspheres to obtain an LiF-rich stabilized SEI. Benefiting from the extensive research on lithium metal anodes in recent years, electrolyte systems suitable for lithium metal anodes were also used in graphite–lithium metal anodes. Lithium salts such as $\text{LiBF}_2(\text{C}_2\text{O}_4)$ - LiBF_4 [122], LiFSI [124,133] were used in composite electrodes and obtained more stable SEI and higher Coulombic efficiency. Zhang et al. [128] used a localized highly concentrated electrolyte to promote more uniform Li deposition, and the full cell matching NCM532 achieved a capacity retention of 80.2% after 500 cycles.

3.5. Carbon Materials in Solid-State Batteries

In lithium metal solid-state batteries, especially inorganic ceramic solid-state batteries, the solid–solid contact between the electrolyte and the two electrodes is poor, and some electrolyte materials have poor compatibility and affinity with lithium metal. In order to obtain a stable structure, the use of carbon materials as interface layers or current collectors can improve the interface stability and affinity of lithium metal anodes with solid electrolytes. Feng et al. [134] obtained a pure air-stable surface on $\text{Li}_{6.75}\text{La}_3\text{Zr}_{1.75}\text{Ta}_{0.25}\text{O}_{12}$ (LLZTO) by thermal decomposition vapor deposition (TVD) (Figure 11a). Benefiting from the amorphous structure of low graphitized carbon (LGC), instantaneous lithiation is achieved, and the impedance of the Li/LLZTO interface is reduced to $9 \Omega \text{ cm}^{-2}$. Chen et al. [135] carbonized a mixture of phenolic resin and polyvinyl butyral on the surface of LLZTO to obtain a porous hard carbon layer (Figure 11b). The multi-layered pore structure of the hard carbon layer provides capillary force and large specific surface area, which, coupled with the chemical reactivity of the carbon material with Li, facilitates the penetration of molten Li with the garnet electrolyte. The Li/LLZTO interface exhibits a low interfacial resistance of $4.7 \Omega \text{ cm}^{-2}$ and a higher critical current density at 40°C . Lee et al. [136] mixed silver and carbon nanoparticles to make anodes, and during the deposition and exfoliation of Li metal, the silver and carbon nanoparticles moved away from the electrolyte and closer

to the electrolyte, respectively (Figure 11c). The gradient electrode structure provides both nucleation sites and interfacial protection layers for Li metal deposition. The pouch cells assembled with silver pyroxene $\text{Li}_6\text{PS}_5\text{Cl}$ exhibited high energy density (900 W h l^{-1}) and superior cycle life (1000 cycles, Coulombic efficiency 99.8%).

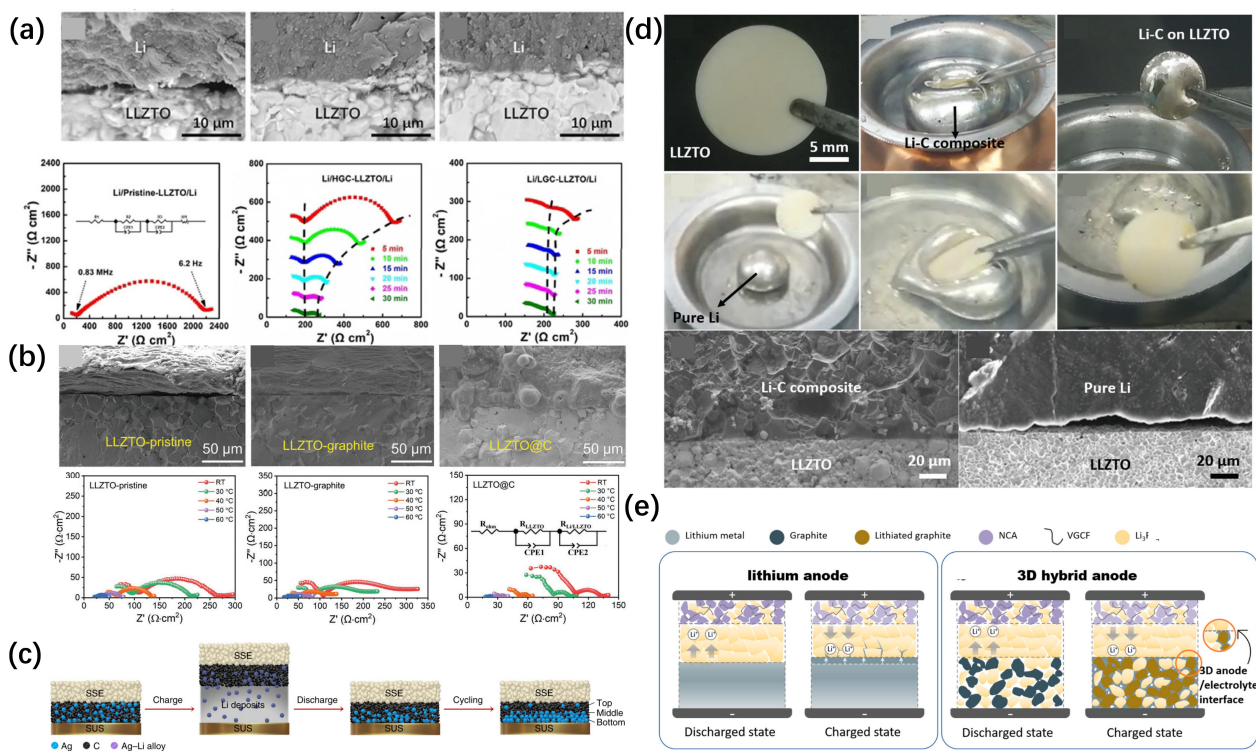


Figure 11. (a) Amorphous low graphitized carbon stabilized Li/LLZTO interface [134]. (b) Li/LLZTO interface stabilized by the porous hard carbon layer [135]. (c) Schematic illustration of the role of the Ag-C nanocomposite layer on the current collector to stabilize the Li coating during charging and discharging [136]. (d) Comparison of the interfacial behavior of LLZTO with pure Li and Li-C [137]. (e) Schematic illustration of the deposition process on Li metal and 3D composite anode in an all-solid-state Li metal battery [138].

In addition, graphite–lithium metal composite electrodes can also be designed using the lithiophilic properties of graphite in solid-state batteries. Duan et al. [137] cast a mixed slurry of lithium metal and graphite into a pole piece and applied it in an LLZO electrolyte battery (Figure 11d). The graphite–lithium metal composite electrode can effectively improve the affinity with the solid electrolyte and reduce the interfacial impedance.

Integrating graphite directly into solid-state electrolytes can utilize the interstitial spaces between graphite and ceramic particles to store lithium metal. Furthermore, the lithium-free negative electrode design can also obtain high specific energy batteries. Ping Liu et al. [138] mixed graphite into the sulfide solid electrolyte, and the resulting composite anode could effectively alleviate the infiltration of lithium metal in the lattice gap and prevent short circuits (Figure 11e). The critical current density of the electrode increases and the interface resistance decreases.

The main problem in organic polymer electrolytes is their low electrical conductivity. Adding fillers can effectively reduce the crystallinity of the electrolyte and improve the conductivity. Materials such as graphene [139,140] and carbon quantum dots [141] as fillers added to polymer electrolytes can simultaneously improve the mechanical properties and electrical conductivity of the electrolytes.

4. Summary and Outlook

Compared with other materials, carbon materials are unique in the field of energy storage due to their low cost, controllable microstructure, tunable electrical conductivity, and modifiable surface structure. Diverse carbon materials have played a huge role in lithium metal batteries. Lithium metal batteries using carbon materials as current collectors can effectively reduce the current density and disperse heat. For the modified carbon material, it will also have the effect of regulating the nucleation and growth of lithium metal. In particular, graphitized carbon materials can be used as a deposition substrate to effectively improve the coulombic efficiency of the anode. The use of carbon materials as additives or artificial SEI in lithium metal batteries can achieve the role of stabilizing the interface layer. In solid-state batteries, carbon materials as interface layers can improve the wettability of lithium metal and electrolyte and increase the ultimate exchange current density. We summarize the application and research of carbon materials in lithium metal batteries in recent years. These works explore the possibilities of carbon materials from various angles. Combined with our reflections on current research, we make some empirical recommendations:

1. When introducing carbon materials into the design of lithium metal batteries, the negative effects of carbon materials, such as chemical/electrochemical stability, structural stability, etc., should be considered at the same time.
2. When designing carbon-based three-dimensional current collectors, the effects of porosity and specific surface area should be considered at the same time. The size of porosity directly affects the mass transfer process of lithium ions: too large porosity will weaken the advantages brought by the 3D structure, while too small porosity will affect the mass transfer process of lithium ions in it. A large specific surface area can achieve more uniform deposition by dispersing the local current density, but at the same time, it will also increase the SEI film area and reduce the first effect and Coulomb efficiency of the battery.
3. The lithium metal foil used in the laboratory test is generally thick. The excessive lithium metal and electrolyte greatly prolong the failure time of the battery. When conducting battery tests, the experimental conditions should be scientifically controlled in order to truly reflect the role of materials in the battery.
4. Pay attention to the overall specific capacity of the battery. Excess lithium metal will reduce the actual specific capacity of the battery. The use of carbon materials can improve the cycle stability and battery life of lithium metal batteries to a certain extent. However, the mass and volume of carbon materials themselves are often overlooked. Controlling the lithium–carbon ratio is particularly important to ensure the specific capacity of the battery.
5. The experiment is established on the basis of the full cell, and its feasibility is verified with a pouch cell or a cylindrical cell.

With the advancement of materials science and the development of nanotechnology, carbon materials are increasingly incorporated into various battery systems and are successfully applied. With the unremitting efforts of mankind, carbon materials will also provide a strong boost to the development of lithium metal batteries.

Author Contributions: Z.W (Zeyu Wu) drafted the majority of this review paper. K.S. and Z.W. (Zhenhua Wang) were involved in the editing and literature-screening efforts. All authors participated in writing the manuscript and discussing the contents to be included in this review. All authors have read and agreed to the published version of the manuscript.

Funding: This research received no external funding.

Data Availability Statement: The data presented in this study are available on request from the corresponding authors.

Conflicts of Interest: The authors declare no conflict of interest.

References

1. Gür, T.M. Review of electrical energy storage technologies, materials and systems: Challenges and prospects for large-scale grid storage. *Energy Environ. Sci.* **2018**, *11*, 2696–2767. [[CrossRef](#)]
2. Goodenough, J.B.; Kim, Y. Challenges for Rechargeable Li Batteries. *Chem. Mater.* **2010**, *22*, 587–603. [[CrossRef](#)]
3. Dunn, B.; Kamath, H.; Tarascon, J.M. Electrical Energy Storage for the Grid: A Battery of Choices. *Science* **2011**, *334*, 928–935. [[CrossRef](#)] [[PubMed](#)]
4. Winter, M.; Barnett, B.; Xu, K. Before Li Ion Batteries. *Chem. Rev.* **2018**, *118*, 11433–11456. [[CrossRef](#)] [[PubMed](#)]
5. Li, M.; Lu, J.; Chen, Z.; Amine, K. 30 Years of Lithium-Ion Batteries. *Adv. Mater.* **2018**, *30*, 1800561. [[CrossRef](#)]
6. Armand, M.; Tarascon, J.M. Building better batteries. *Nature* **2008**, *451*, 652–657. [[CrossRef](#)]
7. Tarascon, J.M.; Armand, M. Issues and challenges facing rechargeable lithium batteries. *Nature* **2001**, *414*, 359–367. [[CrossRef](#)]
8. Liu, W.; Oh, P.; Liu, X.; Lee, M.J.; Cho, W.; Chae, S.; Kim, Y.; Cho, J. Nickel-rich layered lithium transition-metal oxide for high-energy lithium-ion batteries. *Angew. Chem. Int. Ed.* **2015**, *54*, 4440–4457. [[CrossRef](#)]
9. Choi, J.W.; Aurbach, D. Promise and reality of post-lithium-ion batteries with high energy densities. *Nat. Rev. Mater.* **2016**, *1*, 16013. [[CrossRef](#)]
10. Zhang, W.-J. A review of the electrochemical performance of alloy anodes for lithium-ion batteries. *J. Power Sources* **2011**, *196*, 13–24. [[CrossRef](#)]
11. Lin, D.; Liu, Y.; Cui, Y. Reviving the lithium metal anode for high-energy batteries. *Nat. Nanotechnol.* **2017**, *12*, 194–206. [[CrossRef](#)] [[PubMed](#)]
12. Guo, Y.; Li, H.; Zhai, T. Reviving Lithium-Metal Anodes for Next-Generation High-Energy Batteries. *Adv. Mater.* **2017**, *29*, 1700007. [[CrossRef](#)] [[PubMed](#)]
13. Zu, C.-X.; Li, H. Thermodynamic analysis on energy densities of batteries. *Energy Environ. Sci.* **2011**, *4*, 2614–2624. [[CrossRef](#)]
14. Albertus, P.; Babinec, S.; Litzelman, S.; Newman, A. Status and challenges in enabling the lithium metal electrode for high-energy and low-cost rechargeable batteries. *Nat. Energy* **2018**, *3*, 16–21. [[CrossRef](#)]
15. Zhang, H.; Eshetu, G.G.; Judez, X.; Li, C.M.; Rodriguez-Martinez, L.M.; Armand, M. Electrolyte Additives for Lithium Metal Anodes and Rechargeable Lithium Metal Batteries: Progress and Perspectives. *Angew. Chem. Int. Ed.* **2018**, *57*, 15002–15027. [[CrossRef](#)]
16. Chen, S.R.; Zheng, J.M.; Mei, D.H.; Han, K.S.; Engelhard, M.H.; Zhao, W.G.; Xu, W.; Liu, J.; Zhang, J.G. High-Voltage Lithium-Metal Batteries Enabled by Localized High-Concentration Electrolytes. *Adv. Mater.* **2018**, *30*, 1706102. [[CrossRef](#)]
17. Ren, X.D.; Zou, L.F.; Cao, X.; Engelhard, M.H.; Liu, W.; Burton, S.D.; Lee, H.; Niu, C.J.; Matthews, B.E.; Zhu, Z.H.; et al. Enabling High-Voltage Lithium-Metal Batteries under Practical Conditions. *Joule* **2019**, *3*, 1662–1676. [[CrossRef](#)]
18. Qian, J.F.; Henderson, W.A.; Xu, W.; Bhattacharya, P.; Engelhard, M.; Borodin, O.; Zhang, J.G. High rate and stable cycling of lithium metal anode. *Nat. Commun.* **2015**, *6*, 6362. [[CrossRef](#)]
19. Fan, X.L.; Chen, L.; Borodin, O.; Ji, X.; Chen, J.; Hou, S.; Deng, T.; Zheng, J.; Yang, C.Y.; Liou, S.C.; et al. Non-flammable electrolyte enables Li-metal batteries with aggressive cathode chemistries. *Nat. Nanotechnol.* **2018**, *13*, 715–722. [[CrossRef](#)]
20. Suo, L.M.; Xue, W.J.; Gobet, M.; Greenbaum, S.G.; Wang, C.; Chen, Y.M.; Yang, W.L.; Li, Y.X.; Li, J. Fluorine-donating electrolytes enable highly reversible 5-V-class Li metal batteries. *Proc. Natl. Acad. Sci. USA* **2018**, *115*, 1156–1161. [[CrossRef](#)]
21. Ding, F.; Xu, W.; Graff, G.L.; Zhang, J.; Sushko, M.L.; Chen, X.L.; Shao, Y.Y.; Engelhard, M.H.; Nie, Z.M.; Xiao, J.; et al. Dendrite-Free Lithium Deposition via Self-Healing Electrostatic Shield Mechanism. *J. Am. Chem. Soc.* **2013**, *135*, 4450–4456. [[CrossRef](#)]
22. Zhang, S.; Cheng, B.; Fang, Y.; Dang, D.; Shen, X.; Li, Z.; Wu, M.; Hong, Y.; Liu, Q. Inhibition of lithium dendrites and dead lithium by an ionic liquid additive toward safe and stable lithium metal anodes. *Chin. Chem. Lett.* **2022**, *33*, 3951–3954. [[CrossRef](#)]
23. Zhang, W.D.; Tu, Z.Y.; Qian, J.W.; Choudhury, S.; Archer, L.A.; Lu, Y.Y. Design Principles of Functional Polymer Separators for High-Energy, Metal-Based Batteries. *Small* **2018**, *14*, 1703001. [[CrossRef](#)] [[PubMed](#)]
24. Hao, X.M.; Zhu, J.; Jiang, X.; Wu, H.T.; Qiao, J.S.; Sun, W.; Wang, Z.H.; Sun, K.N. Ultrastrong Polyoxazole Nanofiber Membranes for Dendrite-Proof and Heat-Resistant Battery Separators. *Nano Lett.* **2016**, *16*, 2981–2987. [[CrossRef](#)] [[PubMed](#)]
25. Li, C.F.; Liu, S.H.; Shi, C.G.; Liang, G.H.; Lu, Z.T.; Fu, R.W.; Wu, D.C. Two-dimensional molecular brush-functionalized porous bilayer composite separators toward ultrastable high-current density lithium metal anodes. *Nat. Commun.* **2019**, *10*, 1363. [[CrossRef](#)] [[PubMed](#)]
26. Jin, R.; Fu, L.X.; Zhou, H.L.; Wang, Z.Y.; Qiu, Z.F.; Shi, L.Y.; Zhu, J.F.; Yuan, S. High Li⁺ Ionic Flux Separator Enhancing Cycling Stability of Lithium Metal Anode. *ACS Sustain. Chem. Eng.* **2018**, *6*, 2961–2968. [[CrossRef](#)]
27. Woo, S.G.; Hwang, E.K.; Kang, H.K.; Lee, H.; Lee, J.N.; Kim, H.S.; Jeong, G.; Yoo, D.J.; Lee, J.; Kim, S.; et al. High transference number enabled by sulfated zirconia superacid for lithium metal batteries with carbonate electrolytes. *Energy Environ. Sci.* **2021**, *14*, 1420–1428. [[CrossRef](#)]
28. Liu, Y.J.; Tao, X.Y.; Wang, Y.; Jiang, C.; Ma, C.; Sheng, O.W.; Lu, G.X.; Lou, X.W. Self-assembled monolayers direct a LiF-rich interphase toward long-life lithium metal batteries. *Science* **2022**, *375*, 739–745. [[CrossRef](#)] [[PubMed](#)]
29. Yang, Y.; Yao, S.Y.; Liang, Z.W.; Wen, Y.C.; Liu, Z.B.; Wu, Y.W.; Liu, J.; Zhu, M. A Self-Supporting Covalent Organic Framework Separator with Desolvation Effect for High Energy Density Lithium Metal Batteries. *ACS Energy Lett.* **2022**, *7*, 885–896. [[CrossRef](#)]
30. Wu, H.; Jia, H.; Wang, C.; Zhang, J.G.; Xu, W. Recent Progress in Understanding Solid Electrolyte Interphase on Lithium Metal Anodes. *Adv. Energy Mater.* **2020**, *11*, 2003092. [[CrossRef](#)]

31. Meyerson, M.L.; Papa, P.E.; Heller, A.; Mullins, C.B. Recent Developments in Dendrite-Free Lithium-Metal Deposition through Tailoring of Micro- and Nanoscale Artificial Coatings. *ACS Nano* **2021**, *15*, 29–46. [[CrossRef](#)] [[PubMed](#)]
32. Fedorov, R.G.; Maletti, S.; Heubner, C.; Michaelis, A.; Ein-Eli, Y. Molecular Engineering Approaches to Fabricate Artificial Solid-Electrolyte Interphases on Anodes for Li-Ion Batteries: A Critical Review. *Adv. Energy Mater.* **2021**, *11*, 2101173. [[CrossRef](#)]
33. Liu, K.; Pei, A.; Lee, H.R.; Kong, B.; Liu, N.; Lin, D.C.; Liu, Y.Y.; Liu, C.; Hsu, P.C.; Bao, Z.A.; et al. Lithium Metal Anodes with an Adaptive "Solid-Liquid" Interfacial Protective Layer. *J. Am. Chem. Soc.* **2017**, *139*, 4815–4820. [[CrossRef](#)] [[PubMed](#)]
34. Tu, Z.Y.; Choudhury, S.; Zachman, M.J.; Wei, S.Y.; Zhang, K.H.; Kourkoutis, L.F.; Archer, L.A. Designing Artificial Solid-Electrolyte Interphases for Single-Ion and High-Efficiency Transport in Batteries. *Joule* **2017**, *1*, 394–406. [[CrossRef](#)]
35. Gao, Y.; Yan, Z.F.; Gray, J.L.; He, X.; Wang, D.W.; Chen, T.H.; Huang, Q.Q.; Li, Y.G.C.; Wang, H.Y.; Kim, S.H.; et al. Polymer-inorganic solid-electrolyte interphase for stable lithium metal batteries under lean electrolyte conditions. *Nat. Mater.* **2019**, *18*, 384–389. [[CrossRef](#)]
36. Cha, E.; Patel, M.D.; Park, J.; Hwang, J.; Prasad, V.; Cho, K.; Choi, W. 2D MoS₂ as an efficient protective layer for lithium metal anodes in high-performance Li-S batteries. *Nat. Nanotechnol.* **2018**, *13*, 337–344. [[CrossRef](#)]
37. Zheng, G.; Lee, S.W.; Liang, Z.; Lee, H.-W.; Yan, K.; Yao, H.; Wang, H.; Li, W.; Chu, S.; Cui, Y. Interconnected hollow carbon nanospheres for stable lithium metal anodes. *Nat. Nanotechnol.* **2014**, *9*, 618–623. [[CrossRef](#)]
38. Lin, Z.; Ma, Y.; Wang, W.; He, Y.; Wang, M.; Tang, J.; Fan, C.; Sun, K. A homogeneous and mechanically stable artificial diffusion layer using rigid-flexible hybrid polymer for high-performance lithium metal batteries. *J. Energy Chem.* **2022**, *76*, 631–638. [[CrossRef](#)]
39. Han, Y.H.; Jie, Y.L.; Huang, F.Y.; Chen, Y.W.; Lei, Z.W.; Zhang, G.Q.; Ren, X.D.; Qin, L.J.; Cao, R.G.; Jiao, S.H. Enabling Stable Lithium Metal Anode through Electrochemical Kinetics Manipulation. *Adv. Funct. Mater.* **2019**, *29*, 1904629. [[CrossRef](#)]
40. Zhou, B.X.; Bonakdarpour, A.; Stosevski, I.; Fang, B.Z.; Wilkinson, D.P. Modification of Cu current collectors for lithium metal batteries-A review. *Prog. Mater. Sci.* **2022**, *130*, 100996. [[CrossRef](#)]
41. Zhao, H.; Lei, D.N.; He, Y.B.; Yuan, Y.F.; Yun, Q.B.; Ni, B.; Lv, W.; Li, B.H.; Yang, Q.H.; Kang, F.Y.; et al. Compact 3D Copper with Uniform Porous Structure Derived by Electrochemical Dealloying as Dendrite-Free Lithium Metal Anode Current Collector. *Adv. Energy Mater.* **2018**, *8*, 1800266. [[CrossRef](#)]
42. Ke, X.; Liang, Y.H.; Ou, L.H.; Liu, H.D.; Chen, Y.M.; Wu, W.L.; Cheng, Y.F.; Guo, Z.P.; Lai, Y.Q.; Liu, P.; et al. Surface engineering of commercial Ni foams for stable Li metal anodes. *Energy Stor. Mater.* **2019**, *23*, 547–555. [[CrossRef](#)]
43. Fan, L.; Wei, S.Y.; Li, S.Y.; Li, Q.; Lu, Y.Y. Recent Progress of the Solid-State Electrolytes for High-Energy Metal-Based Batteries. *Adv. Energy Mater.* **2018**, *8*, 1702657. [[CrossRef](#)]
44. Yang, C.P.; Fu, K.; Zhang, Y.; Hitz, E.; Hu, L.B. Protected Lithium-Metal Anodes in Batteries: From Liquid to Solid. *Adv. Mater.* **2017**, *29*, 1701169. [[CrossRef](#)]
45. Zhou, D.; Shanmukaraj, D.; Tkacheva, A.; Armand, M.; Wang, G.X. Polymer Electrolytes for Lithium-Based Batteries: Advances and Prospects. *Chem* **2019**, *5*, 2326–2352. [[CrossRef](#)]
46. Chen, R.S.; Li, Q.H.; Yu, X.Q.; Chen, L.Q.; Li, H. Approaching Practically Accessible Solid-State Batteries: Stability Issues Related to Solid Electrolytes and Interfaces. *Chem. Rev.* **2020**, *120*, 6820–6877. [[CrossRef](#)]
47. Yu, Q.J.; Jiang, K.C.; Yu, C.L.; Chen, X.J.; Zhang, C.J.; Yao, Y.; Jiang, B.; Long, H.J. Recent progress of composite solid polymer electrolytes for all-solid-state lithium metal batteries. *Chin. Chem. Lett.* **2021**, *32*, 2659–2678. [[CrossRef](#)]
48. Zhao, B.L.; Ma, L.X.; Wu, K.; Cao, M.X.; Xu, M.G.; Zhang, X.X.; Liu, W.; Chen, J.T. Asymmetric double-layer composite electrolyte with enhanced ionic conductivity and interface stability for all-solid-state lithium metal batteries. *Chin. Chem. Lett.* **2021**, *32*, 125–131. [[CrossRef](#)]
49. Liu, H.; Cheng, X.B.; Huang, J.Q.; Yuan, H.; Lu, Y.; Yan, C.; Zhu, G.L.; Xu, R.; Zhao, C.Z.; Hou, L.P.; et al. Controlling Dendrite Growth in Solid-State Electrolytes. *ACS Energy Lett.* **2020**, *5*, 833–843. [[CrossRef](#)]
50. Sun, M.H.; Liu, T.F.; Yuan, Y.F.; Ling, M.; Xu, N.; Liu, Y.Y.; Yan, L.J.; Li, H.; Liu, C.Y.; Lu, Y.Y.; et al. Visualizing Lithium Dendrite Formation within Solid-State Electrolytes. *ACS Energy Lett.* **2021**, *6*, 451–458. [[CrossRef](#)]
51. Raj, V.; Venturi, V.; Kankanallu, V.R.; Kuiri, B.; Viswanathan, V.; Aetukuri, N.P.B. Direct correlation between void formation and lithium dendrite growth in solid-state electrolytes with interlayers. *Nat. Mater.* **2022**, *21*, 1050–1056. [[CrossRef](#)] [[PubMed](#)]
52. Yan, K.; Lu, Z.; Lee, H.-W.; Xiong, F.; Hsu, P.-C.; Li, Y.; Zhao, J.; Chu, S.; Cui, Y. Selective deposition and stable encapsulation of lithium through heterogeneous seeded growth. *Nat. Energy* **2016**, *1*, 16010. [[CrossRef](#)]
53. Pei, A.; Zheng, G.Y.; Shi, F.F.; Li, Y.Z.; Cui, Y. Nanoscale Nucleation and Growth of Electrodeposited Lithium Metal. *Nano Lett.* **2017**, *17*, 1132–1139. [[CrossRef](#)]
54. Jaeckle, M.; Gross, A. Microscopic properties of lithium, sodium, and magnesium battery anode materials related to possible dendrite growth. *J. Chem. Phys.* **2014**, *141*, 174710. [[CrossRef](#)]
55. Xiao, J. How lithium dendrites form in liquid batteries. *Science* **2019**, *366*, 426–427. [[CrossRef](#)] [[PubMed](#)]
56. Cheng, X.B.; Zhang, R.; Zhao, C.Z.; Zhang, Q. Toward Safe Lithium Metal Anode in Rechargeable Batteries: A Review. *Chem. Rev.* **2017**, *117*, 10403–10473. [[CrossRef](#)] [[PubMed](#)]
57. Fleury, V.; Chazalviel, J.N.; Rosso, M.; Sapoval, B. The role of the anions in the growth speed of fractal electrodeposits. *J. Electroanal. Chem. Interfacial Electrochem.* **1990**, *290*, 249–255. [[CrossRef](#)]
58. Chazalviel, J. Electrochemical aspects of the generation of ramified metallic electrodeposits. *Phys. Rev. A* **1990**, *42*, 7355–7367. [[CrossRef](#)]

59. Seong, I.W.; Hong, C.H.; Kim, B.K.; Yoon, W.Y. The effects of current density and amount of discharge on dendrite formation in the lithium powder anode electrode. *J. Power Sources* **2008**, *178*, 769–773. [[CrossRef](#)]
60. Monroe, C.; Newman, J. The impact of elastic deformation on deposition kinetics at lithium/polymer interfaces. *J. Electrochem. Soc.* **2005**, *152*, A396–A404. [[CrossRef](#)]
61. Ota, H.; Shima, K.; Ue, M.; Yamaki, J. Effect of vinylene carbonate as additive to electrolyte for lithium metal anode. *Electrochim. Acta* **2004**, *49*, 565–572. [[CrossRef](#)]
62. Fang, C.C.; Li, J.X.; Zhang, M.H.; Zhang, Y.H.; Yang, F.; Lee, J.Z.; Lee, M.H.; Alvarado, J.; Schroeder, M.A.; Yang, Y.Y.C.; et al. Quantifying inactive lithium in lithium metal batteries. *Nature* **2019**, *572*, 511–515. [[CrossRef](#)] [[PubMed](#)]
63. Xiang, Y.; Tao, M.; Zhong, G.; Liang, Z.; Zheng, G.; Huang, X.; Liu, X.; Jin, Y.; Xu, N.; Armand, M.; et al. Quantitatively analyzing the failure processes of rechargeable Li metal batteries. *Sci. Adv.* **2021**, *7*, eabj3423. [[CrossRef](#)] [[PubMed](#)]
64. Cheng, X.B.; Zhang, R.; Zhao, C.Z.; Wei, F.; Zhang, J.G.; Zhang, Q. A Review of Solid Electrolyte Interphases on Lithium Metal Anode. *Adv. Sci.* **2016**, *3*, 1500213. [[CrossRef](#)]
65. Xu, K. Electrolytes and Interphases in Li-Ion Batteries and Beyond. *Chem. Rev.* **2014**, *114*, 11503–11618. [[CrossRef](#)]
66. Cohen, Y.S.; Cohen, Y.; Aurbach, D. Micromorphological studies of lithium electrodes in alkyl carbonate solutions using in situ atomic force microscopy. *J. Phys. Chem. B* **2000**, *104*, 12282–12291. [[CrossRef](#)]
67. An, S.J.; Li, J.; Daniel, C.; Mohanty, D.; Nagpure, S.; Wood, D.L., III. The state of understanding of the lithium-ion-battery graphite solid electrolyte interphase (SEI) and its relationship to formation cycling. *Carbon* **2016**, *105*, 52–76. [[CrossRef](#)]
68. Aurbach, D.; Daroux, M.L.; Faguy, P.W.; Yeager, E. IDENTIFICATION OF SURFACE-FILMS FORMED ON LITHIUM IN PROPYLENE CARBONATE SOLUTIONS. *J. Electrochem. Soc.* **1987**, *134*, 1611–1620. [[CrossRef](#)]
69. Aurbach, D.; Zaban, A.; Ein-Eli, Y.; Weissman, I.; Chusid, O.; Markovsky, B.; Levi, M.; Levi, E.; Schechter, A.; Granot, E. Recent studies on the correlation between surface chemistry, morphology, three-dimensional structures and performance of Li and Li-C intercalation anodes in several important electrolyte systems. *J. Power Sources* **1997**, *68*, 91–98. [[CrossRef](#)]
70. Aurbach, D.; Zaban, A.; Gofer, Y.; Ely, Y.E.; Weissman, I.; Chusid, O.; Abramson, O. Recent studies of the lithium liquid electrolyte interface-electrochemical, morphological and spectral studies of a few important systems. *J. Power Sources* **1995**, *54*, 76–84. [[CrossRef](#)]
71. Aurbach, D. Review of selected electrode-solution interactions which determine the performance of Li and Li ion batteries. *J. Power Sources* **2000**, *89*, 206–218. [[CrossRef](#)]
72. Peled, E.; Ardel, G. Advanced Model for Solid Electrolyte Interphase Electrodes in Liquid and Polymer Electrolytes. *J. Electrochem. Soc.* **1997**, *144*, L208–L210. [[CrossRef](#)]
73. Li, Y.; Li, Y.; Pei, A.; Yan, K.; Sun, Y.; Wu, C.-L.; Joubert, L.-M.; Chin, R.; Koh, A.L.; Yu, Y.; et al. Atomic structure of sensitive battery materials and Interfaces revealed by cryo-electron microscopy. *Science* **2017**, *358*, 506–510. [[CrossRef](#)] [[PubMed](#)]
74. Ramasubramanian, A.; Yurkiv, V.; Foroozan, T.; Ragone, M.; Shahbazian-Yassar, R.; Mashayek, F.I. Lithium Diffusion Mechanism through Solid-Electrolyte Interphase in Rechargeable Lithium Batteries. *J. Phys. Chem. C* **2019**, *123*, 10237–10245. [[CrossRef](#)]
75. Zhang, X.Q.; Cheng, X.B.; Chen, X.; Yan, C.; Zhang, Q. Fluoroethylene Carbonate Additives to Render Uniform Li Deposits in Lithium Metal Batteries. *Adv. Funct. Mater.* **2017**, *27*, 1605989. [[CrossRef](#)]
76. Mogi, R.; Inaba, M.; Jeong, S.K.; Iriyama, Y.; Abe, T.; Ogumi, Z. Effects of some organic additives on lithium deposition in propylene carbonate. *J. Electrochem. Soc.* **2002**, *149*, A1578–A1583. [[CrossRef](#)]
77. Mukra, T.; Peled, E. Elucidation of the Losses in Cycling Lithium-Metal Anodes in Carbonate-Based Electrolytes. *J. Electrochem. Soc.* **2020**, *167*, 100520. [[CrossRef](#)]
78. Zhang, M.S.; Liu, R.J.; Wang, Z.K.; Xing, X.Y.; Liu, Y.G.; Deng, B.B.; Yang, T. Electrolyte additive maintains high performance for dendrite-free lithium metal anode. *Chin. Chem. Lett.* **2020**, *31*, 1217–1220. [[CrossRef](#)]
79. Cheng, X.B.; Zhao, M.Q.; Chen, C.; Pentecost, A.; Maleski, K.; Mathis, T.; Zhang, X.Q.; Zhang, Q.; Jiang, J.J.; Gogotsi, Y. Nanodiamonds suppress the growth of lithium dendrites. *Nat. Commun.* **2017**, *8*, 336. [[CrossRef](#)]
80. Hu, Y.; Chen, W.; Lei, T.; Jiao, Y.; Wang, H.; Wang, X.; Rao, G.; Wang, X.; Chen, B.; Xiong, J. Graphene Quantum Dots as the Nucleation Sites and Interfacial Regulator to Suppress Lithium Dendrites for High-Loading Lithium-Sulfur Battery. *Nano Energy* **2019**, *68*, 104373. [[CrossRef](#)]
81. Xu, S.; Zhao, T.; Ye, Y.; Yang, T.; Luo, R.; Li, L.; Wu, F.; Chen, R. A Designed Lithiophilic Carbon Channel on Separator to Regulate Lithium Deposition Behavior. *Small* **2022**, *18*, 2104390. [[CrossRef](#)] [[PubMed](#)]
82. Li, Z.; Peng, M.; Zhou, X.; Shin, K.; Tunmee, S.; Zhang, X.; Xie, C.; Saitoh, H.; Zheng, Y.; Zhou, Z.; et al. In Situ Chemical Lithiation Transforms Diamond-Like Carbon into an Ultrastrong Ion Conductor for Dendrite-Free Lithium-Metal Anodes. *Adv. Mater.* **2021**, *33*, 2100793. [[CrossRef](#)] [[PubMed](#)]
83. Wang, Z.H.; Wang, X.D.; Sun, W.; Sun, K.N. Dendrite-Free Lithium Metal Anodes in High Performance Lithium-Sulfur Batteries with Bifunctional Carbon Nanofiber Interlayers. *Electrochim. Acta* **2017**, *252*, 127–137. [[CrossRef](#)]
84. Liu, Y.; Liu, Q.; Xin, L.; Liu, Y.; Yang, F.; Stach, E.A.; Xie, J. Making Li-metal electrodes rechargeable by controlling the dendrite growth direction. *Nat. Energy* **2017**, *2*, 17083. [[CrossRef](#)]
85. Wondimkun, Z.T.; Beyene, T.T.; Weret, M.A.; Sahalie, N.A.; Huang, C.-J.; Thirumalraj, B.; Jote, B.A.; Wang, D.; Su, W.-N.; Wang, C.-H.; et al. Binder-free ultra-thin graphene oxide as an artificial solid electrolyte interphase for anode-free rechargeable lithium metal batteries. *J. Power Sources* **2020**, *450*, 227589. [[CrossRef](#)]

86. Liu, W.; Xia, Y.; Wang, W.; Wang, Y.; Jin, J.; Chen, Y.; Paek, E.; Mitlin, D. Pristine or Highly Defective? Understanding the Role of Graphene Structure for Stable Lithium Metal Plating. *Adv. Energy Mater.* **2019**, *9*, 1802918. [[CrossRef](#)]
87. Ma, Y.; Qi, P.; Ma, J.; Wei, L.; Zhao, L.; Cheng, J.; Su, Y.; Gu, Y.; Lian, Y.; Peng, Y.; et al. Wax-Transferred Hydrophobic CVD Graphene Enables Water-Resistant and Dendrite-Free Lithium Anode toward Long Cycle Li-Air Battery. *Adv. Sci.* **2021**, *8*, 2100488. [[CrossRef](#)] [[PubMed](#)]
88. Zhou, Y.; Zhang, X.; Ding, Y.; Zhang, L.; Yu, G. Reversible Deposition of Lithium Particles Enabled by Ultraconformal and Stretchable Graphene Film for Lithium Metal Batteries. *Adv. Mater.* **2020**, *32*, 2005763. [[CrossRef](#)]
89. Xie, K.; Wei, W.; Yuan, K.; Lu, W.; Guo, M.; Li, Z.; Song, Q.; Liu, X.; Wang, J.-G.; Shen, C. Toward Dendrite-Free Lithium Deposition via Structural and Interfacial Synergistic Effects of 3D Graphene@Ni Scaffold. *ACS Appl. Mater. Interfaces* **2016**, *8*, 26091–26097. [[CrossRef](#)]
90. Fan, L.; Sun, B.; Yan, K.; Xiong, P.; Guo, X.; Guo, Z.; Zhang, N.; Feng, Y.; Sun, K.; Wang, G. A Dual-Protective Artificial Interface for Stable Lithium Metal Anodes. *Adv. Energy Mater.* **2021**, *11*, 2102242. [[CrossRef](#)]
91. Zhu, J.; Li, P.; Chen, X.; Legut, D.; Fan, Y.; Zhang, R.; Lu, Y.; Cheng, X.; Zhang, Q. Rational design of graphitic-inorganic Bi-layer artificial SEI for stable lithium metal anode. *Energy Stor. Mater.* **2019**, *16*, 426–433. [[CrossRef](#)]
92. Tang, K.; Xiao, J.; Li, X.; Wang, D.; Long, M.; Chen, J.; Gao, H.; Chen, W.; Liu, C.; Liu, H. Advances of Carbon-Based Materials for Lithium Metal Anodes. *Front. Chem.* **2020**, *8*, 595972. [[CrossRef](#)] [[PubMed](#)]
93. Pomerantseva, E.; Bonaccorso, F.; Feng, X.; Cui, Y.; Gogotsi, Y. Energy storage: The future enabled by nanomaterials. *Science* **2019**, *366*, 969–980. [[CrossRef](#)] [[PubMed](#)]
94. Cao, W.; Chen, W.; Lu, M.; Zhang, C.; Tian, D.; Wang, L.; Yu, F. In situ generation of Li₃N concentration gradient in 3D carbon-based lithium anodes towards highly-stable lithium metal batteries. *J. Energy Chem.* **2022**, *76*, 648–656. [[CrossRef](#)]
95. Liu, J.; Ma, H.; Wen, Z.; Li, H.; Yang, J.; Pei, N.; Zhang, P.; Zhao, J. Layered Ag-graphene films synthesized by Gamma ray irradiation for stable lithium metal anodes in carbonate-based electrolytes. *J. Energy Chem.* **2022**, *64*, 354–363. [[CrossRef](#)]
96. Chen, H.; Li, M.; Li, C.; Li, X.; Wu, Y.; Chen, X.; Wu, J.; Li, X.; Chen, Y. Electrospun carbon nanofibers for lithium metal anodes: Progress and perspectives. *Chin. Chem. Lett.* **2022**, *33*, 141–152. [[CrossRef](#)]
97. Zhang, Z.; Zhu, P.; Li, C.; Yu, J.; Cai, J.; Yang, Z. Needle-like cobalt phosphide arrays grown on carbon fiber cloth as a binder-free electrode with enhanced lithium storage performance. *Chin. Chem. Lett.* **2021**, *32*, 154–157. [[CrossRef](#)]
98. Liu, H.; Zhang, J.; Liu, Y.; Wei, Y.; Ren, S.; Pan, L.; Su, Y.; Xiao, J.; Fan, H.; Lin, Y.; et al. A flexible artificial solid-electrolyte interlayer supported by compactness-tailored carbon nanotube network for dendrite-free lithium metal anode. *J. Energy Chem.* **2022**, *69*, 421–427. [[CrossRef](#)]
99. Zhang, F.; Liu, X.Y.; Yang, M.H.; Cao, X.Q.; Huang, X.Y.; Tian, Y.; Zhang, F.; Li, H.X. Novel S-doped ordered mesoporous carbon nanospheres toward advanced lithium metal anodes. *Nano Energy* **2020**, *69*, 104443. [[CrossRef](#)]
100. Qi, J.; Li, Y.; Wei, G.; Li, J.; Sun, X.; Shen, J.; Han, W.; Wang, L. Nitrogen doped porous hollow carbon spheres for enhanced benzene removal. *Sep. Purif. Technol.* **2017**, *188*, 112–118. [[CrossRef](#)]
101. Jiang, H.; Zhou, Y.; Zhu, H.; Qin, F.; Han, Z.; Bai, M.; Yang, J.; Li, J.; Hong, B.; Lai, Y. Interconnected stacked hollow carbon spheres uniformly embedded with Ni₂P nanoparticles as scalable host for practical Li metal anode. *Chem. Eng. J.* **2022**, *428*, 132648. [[CrossRef](#)]
102. Chen, W.; Hong, Y.; Zhao, Z.; Zhang, Y.; Pan, L.; Wan, J.; Nazir, M.; Wang, J.; He, H. Directing the deposition of lithium metal to the inner concave surface of graphitic carbon tubes to enable lithium-metal batteries. *J. Mater. Chem. A* **2021**, *9*, 16936–16942. [[CrossRef](#)]
103. Liu, L.; Yin, Y.-X.; Li, J.-Y.; Li, N.-W.; Zeng, X.-X.; Ye, H.; Guo, Y.-G.; Wan, L.-J. Free-Standing Hollow Carbon Fibers as High-Capacity Containers for Stable Lithium Metal Anodes. *Joule* **2017**, *1*, 563–575. [[CrossRef](#)]
104. Chen, C.; Guan, J.; Li, N.W.; Lu, Y.; Luan, D.; Zhang, C.H.; Cheng, G.; Yu, L.; Lou, X.W.D. Lotus-Root-Like Carbon Fibers Embedded with Ni-Co Nanoparticles for Dendrite-Free Lithium Metal Anodes. *Adv. Mater.* **2021**, *33*, 2100608. [[CrossRef](#)]
105. Wang, Z.Y.; Lu, Z.X.; Guo, W.; Luo, Q.; Yin, Y.H.; Liu, X.B.; Li, Y.S.; Xia, B.Y.; Wu, Z.P. A Dendrite-Free Lithium/Carbon Nanotube Hybrid for Lithium-Metal Batteries. *Adv. Mater.* **2021**, *33*, 2006702. [[CrossRef](#)]
106. Niu, C.J.; Pan, H.L.; Xu, W.; Xiao, J.; Zhang, J.G.; Luo, L.L.; Wang, C.M.; Mei, D.H.; Meng, J.S.; Wang, X.P.; et al. Self-smoothing anode for achieving high-energy lithium metal batteries under realistic conditions. *Nat. Nanotechnol.* **2019**, *14*, 594–601. [[CrossRef](#)]
107. Liu, K.; Li, Z.; Xie, W.; Li, J.; Rao, D.; Shao, M.; Zhang, B.; Wei, M. Oxygen-rich carbon nanotube networks for enhanced lithium metal anode. *Energy Stor. Mater.* **2018**, *15*, 308–314. [[CrossRef](#)]
108. Lin, D.; Liu, Y.; Liang, Z.; Lee, H.-W.; Sun, J.; Wang, H.; Yan, K.; Xie, J.; Cui, Y. Layered reduced graphene oxide with nanoscale interlayer gaps as a stable host for lithium metal anodes. *Nat. Nanotechnol.* **2016**, *11*, 626–632. [[CrossRef](#)]
109. Xu, Z.; Xu, L.; Xu, Z.; Deng, Z.; Wang, X. N, O-Codoped Carbon Nanosheet Array Enabling Stable Lithium Metal Anode. *Adv. Funct. Mater.* **2021**, *31*, 2102354. [[CrossRef](#)]
110. Wang, T.; Zhai, P.; Legut, D.; Wang, L.; Liu, X.; Li, B.; Dong, C.; Fan, Y.; Gong, Y.; Zhang, Q. S-Doped Graphene-Regional Nucleation Mechanism for Dendrite-Free Lithium Metal Anodes. *Adv. Energy Mater.* **2019**, *9*, 1804000. [[CrossRef](#)]
111. Li, Z.; Li, X.; Zhou, L.; Xiao, Z.; Zhou, S.; Zhang, X.; Li, L.; Zhi, L. A synergistic strategy for stable lithium metal anodes using 3D fluorine-doped graphene shuttle-implanted porous carbon networks. *Nano Energy* **2018**, *49*, 179–185. [[CrossRef](#)]
112. Fang, Y.; Zeng, Y.; Jin, Q.; Lu, X.F.; Luan, D.; Zhang, X.; Lou, X.W.D. Nitrogen-Doped Amorphous Zn-Carbon Multichannel Fibers for Stable Lithium Metal Anodes. *Angew. Chem. Int. Ed.* **2021**, *60*, 8515–8520. [[CrossRef](#)] [[PubMed](#)]

113. Yang, T.; Li, L.; Wu, F.; Chen, R. A Soft Lithiophilic Graphene Aerogel for Stable Lithium Metal Anode. *Adv. Funct. Mater.* **2020**, *30*, 2002013. [[CrossRef](#)]
114. Zhao, C.; Yu, C.; Li, S.; Guo, W.; Zhao, Y.; Dong, Q.; Lin, X.; Song, Z.; Tan, X.; Wang, C.; et al. Ultrahigh-Capacity and Long-Life Lithium-Metal Batteries Enabled by Engineering Carbon Nanofiber-Stabilized Graphene Aerogel Film Host. *Small* **2018**, *14*, 1803310. [[CrossRef](#)]
115. Li, Y.; Li, Y.; Zhang, L.; Tao, H.; Li, Q.; Zhang, J.; Yang, X. Lithiophilicity: The key to efficient lithium metal anodes for lithium batteries. *J. Energy Chem.* **2022**, *in press*. [[CrossRef](#)]
116. Zhang, F.; Liu, P.; Tian, Y.; Wu, J.; Wang, X.; Li, H.; Liu, X. Uniform lithium nucleation/deposition regulated by N/S co-doped carbon nanospheres towards ultra-stable lithium metal anodes. *J. Mater. Chem. A* **2022**, *10*, 1463–1472. [[CrossRef](#)]
117. Zhao, C.Y.; Yin, X.J.; Guo, Z.K.; Zhao, D.; Yang, G.Y.; Chen, A.S.; Fan, L.S.; Zhang, Y.; Zhang, N.Q. High lithiophilic nitrogen-doped carbon nanotube arrays prepared by in-situ catalyze for lithium metal anode. *Chin. Chem. Lett.* **2021**, *32*, 2254–2258. [[CrossRef](#)]
118. Chu, Y.T.; Xi, B.J.; Xiong, S.L. One-step construction of MoO₂ uniform nanoparticles on graphene with enhanced lithium storage. *Chin. Chem. Lett.* **2021**, *32*, 1983–1987. [[CrossRef](#)]
119. Li, D.; Gao, Y.; Xie, C.; Zheng, Z. Au-coated carbon fabric as Janus current collector for dendrite-free flexible lithium metal anode and battery. *Appl. Phys. Rev.* **2022**, *9*, 011424. [[CrossRef](#)]
120. Tian, R.; Wan, S.L.; Guan, L.; Duan, H.N.; Guo, Y.P.; Li, H.; Liu, H.Z. Oriented growth of Li metal for stable Li/carbon composite negative electrode. *Electrochim. Acta* **2018**, *292*, 227–233. [[CrossRef](#)]
121. Gao, Y.; Wang, D.; Shin, Y.K.; Yan, Z.; Han, Z.; Wang, K.; Hossain, M.J.; Shen, S.; AlZahrani, A.; van Duin, A.C.T.; et al. Stable metal anodes enabled by a labile organic molecule bonded to a reduced graphene oxide aerogel. *Proc. Natl. Acad. Sci. USA* **2020**, *117*, 30135–30141. [[CrossRef](#)]
122. Martin, C.; Genovese, M.; Louli, A.J.; Weber, R.; Dahn, J.R. Cycling Lithium Metal on Graphite to Form Hybrid Lithium-Ion/Lithium Metal Cells. *Joule* **2020**, *4*, 1296–1310. [[CrossRef](#)]
123. Duan, J.; Zheng, Y.; Luo, W.; Wu, W.; Wang, T.; Xie, Y.; Li, S.; Li, J.; Huang, Y. Is graphite lithiophobic or lithiophilic? *Natl. Sci. Rev.* **2020**, *7*, 1208–1217. [[CrossRef](#)] [[PubMed](#)]
124. Yang, G.; Zhang, S.; Weng, S.; Li, X.; Wang, X.; Wang, Z.; Chen, L. Anionic Effect on Enhancing the Stability of a Solid Electrolyte Interphase Film for Lithium Deposition on Graphite. *Nano Lett.* **2021**, *21*, 5316–5323. [[CrossRef](#)] [[PubMed](#)]
125. Ye, H.; Xin, S.; Yin, Y.-X.; Li, J.-Y.; Guo, Y.-G.; Wan, L.-J. Stable Li Plating/Stripping Electrochemistry Realized by a Hybrid Li Reservoir in Spherical Carbon Granules with 3D Conducting Skeletons. *J. Am. Chem. Soc.* **2017**, *139*, 5916–5922. [[CrossRef](#)]
126. Sun, Y.; Zheng, G.; Seh, Z.W.; Liu, N.; Wang, S.; Sun, J.; Lee, H.R.; Cui, Y. Graphite-Encapsulated Li-Metal Hybrid Anodes for High-Capacity Li Batteries. *Chem* **2016**, *1*, 287–297. [[CrossRef](#)]
127. Zuo, T.T.; Wu, X.W.; Yang, C.P.; Yin, Y.X.; Ye, H.; Li, N.W.; Guo, Y.G. Graphitized Carbon Fibers as Multifunctional 3D Current Collectors for High Areal Capacity Li Anodes. *Adv. Mater.* **2017**, *29*, 1700389. [[CrossRef](#)]
128. Cai, W.; Yan, C.; Yao, Y.X.; Xu, L.; Chen, X.R.; Huang, J.Q.; Zhang, Q. The Boundary of Lithium Plating in Graphite Electrode for Safe Lithium-Ion Batteries. *Angew. Chem. Int. Ed.* **2021**, *60*, 13007–13012. [[CrossRef](#)]
129. Yang, G.; Zhang, S.; Tong, Y.; Li, X.; Wang, Z.; Chen, L. Minimizing carbon particle size to improve lithium deposition on natural graphite. *Carbon* **2019**, *155*, 9–15. [[CrossRef](#)]
130. Ho, A.S.; Parkinson, D.Y.; Finegan, D.P.; Trask, S.E.; Jansen, A.N.; Tong, W.; Balsara, N.P. 3D Detection of Lithiation and Lithium Plating in Graphite Anodes during Fast Charging. *ACS Nano* **2021**, *15*, 10480–10487. [[CrossRef](#)]
131. Luo, J.; Wu, C.E.; Su, L.Y.; Huang, S.S.; Fang, C.C.; Wu, Y.S.; Chou, J.; Wu, N.L. A proof-of-concept graphite anode with a lithium dendrite suppressing polymer coating. *J. Power Sources* **2018**, *406*, 63–69. [[CrossRef](#)]
132. Cui, C.; Yang, C.; Eidson, N.; Chen, J.; Han, F.; Chen, L.; Luo, C.; Wang, P.F.; Fan, X.; Wang, C. A Highly Reversible, Dendrite-Free Lithium Metal Anode Enabled by a Lithium-Fluoride-Enriched Interphase. *Adv. Mater.* **2020**, *32*, 1906427. [[CrossRef](#)] [[PubMed](#)]
133. Wang, S.; Liu, D.; Cai, X.; Zhang, L.; Liu, Y.; Qin, X.; Zhao, R.; Zeng, X.; Han, C.; Zhan, C.; et al. Promoting the reversibility of lithium ion/lithium metal hybrid graphite anode by regulating solid electrolyte interface. *Nano Energy* **2021**, *90*, 106510. [[CrossRef](#)]
134. Feng, W.; Dong, X.; Zhang, X.; Lai, Z.; Li, P.; Wang, C.; Wang, Y.; Xia, Y. Li/Garnet Interface Stabilization by Thermal-Decomposition Vapor Deposition of an Amorphous Carbon Layer. *Angew. Chem. Int. Ed.* **2020**, *59*, 5346–5349. [[CrossRef](#)] [[PubMed](#)]
135. Chen, L.; Zhang, J.; Tong, R.A.; Zhang, J.; Wang, H.; Shao, G.; Wang, C.A. Excellent Li/Garnet Interface Wettability Achieved by Porous Hard Carbon Layer for Solid State Li Metal Battery. *Small* **2022**, *18*, 2106142. [[CrossRef](#)] [[PubMed](#)]
136. Lee, Y.G.; Fujiki, S.; Jung, C.; Suzuki, N.; Yashiro, N.; Omoda, R.; Ko, D.S.; Shiratsuchi, T.; Sugimoto, T.; Ryu, S.; et al. High-energy long-cycling all-solid-state lithium metal batteries enabled by silver-carbon composite anodes. *Nat. Energy* **2020**, *5*, 299–308. [[CrossRef](#)]
137. Duan, J.; Wu, W.Y.; Nolan, A.M.; Wang, T.R.; Wen, J.Y.; Hu, C.C.; Mo, Y.F.; Luo, W.; Huang, Y.H. Lithium-Graphite Paste: An Interface Compatible Anode for Solid-State Batteries. *Adv. Mater.* **2019**, *31*, 1807243. [[CrossRef](#)]
138. Xing, X.; Li, Y.; Wang, S.; Liu, H.; Wu, Z.; Yu, S.; Holoubek, J.; Zhou, H.; Liu, P. YY Graphite-Based Lithium-Free 3D Hybrid Anodes for High Energy Density All-Solid-State Batteries. *ACS Energy Lett.* **2021**, *6*, 1831–1838. [[CrossRef](#)]

139. Bao, W.; Hu, Z.Y.; Wang, Y.Y.; Jiang, J.H.; Huo, S.K.; Fan, W.Z.; Chen, W.J.; Jing, X.; Long, X.Y.; Zhang, Y.F. Poly(ionic liquid)-functionalized graphene oxide towards ambient temperature operation of all-solid-state PEO-based polymer electrolyte lithium metal batteries. *Chem. Eng. J.* **2022**, *437*, 135420. [[CrossRef](#)]
140. Nicotera, I.; Simari, C.; Agostini, M.; Enotiadis, A.; Brutti, S. A Novel Li+-Nafion-Sulfonated Graphene Oxide Membrane as Single Lithium-Ion Conducting Polymer Electrolyte for Lithium Batteries. *J. Phys. Chem. C* **2019**, *123*, 27406–27416. [[CrossRef](#)]
141. Li, Z.Y.; Liu, F.; Chen, S.S.; Zhai, F.; Li, Y.; Feng, Y.Y.; Feng, W. Single Li ion conducting solid-state polymer electrolytes based on carbon quantum dots for Li-metal batteries. *Nano Energy* **2021**, *82*, 105698. [[CrossRef](#)]